AD

PSDC-TR-25

A PRELIMINARY INVESTIGATION OF "IN-AND-DOWN" AND "IN-AND-UP" RADIATION COMPONENTS

October 1966

Technical Report Prepared for

Office of Civil Defense
Office of the Secretary of the Army
Washington, D.C. 20310

Through

The Protective Structures Development Center
Joint Civil Defense Support Group
Fort Belvoir, Virginia

By

CONESCO, A Division of Flow Corporation
Watertown, Massachusetts
Contract No. DA-18-020-ENG-3407
Work Order (OCD)-PS-65-17
Subtask 1117A

79

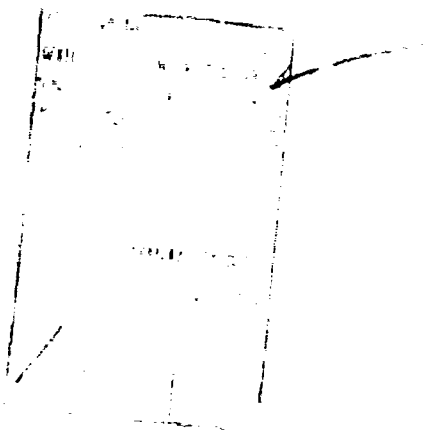

OCD REVIEW NOTICE

"This report has been reviewed in the Office of Civil Defense and approved for publication. Approval does not signify that the contents necessarily reflect the views and policies of the Office of Civil Defense."

Destroy this report when no longer needed.
Do not return it to the originator.

DETACHABLE

SUMMARY OF REPORT NO. PSDC-TR-25 A PRELIMINARY INVESTIGATION OF "IN-AND-DOWN" AND "IN-AND-UP" RADIATION COMPONENTS

October 1966

Technical Report Prepared for

Office of Civil Defense
Office of the Secretary of the Army
Washington, D.C. 20310

Through

The Protective Structures Development Center
Joint Civil Defense Support Group
Fort Belvoir, Virginia

By

CONESCO, A Division of Flow Corporation
Watertown, Massachusetts
Contract No. DA-18-020-ENG-3407
Work Order (OCD)-PS-65-17
Subtask 1117A

This is a summary of a report which has been reviewed in the Office of Civil Defense and approved for publication. Approval does not signify that the contents necessarily reflect the views and policies of the Office of Civil Defense.

o

SUMMARY

The technology of shelter calculation from fallout radiation has advanced in recent years, justifying confidence in protection factors computed for above-ground locations in simple, "box-type" structures exposed to an infinite field of ground contamination. For other situations, such as the basement of a structure or when a field of contamination is not infinite, either experimental data did not agree well with computed values or the experimental data, usually obtained from complex structures, failed to indicate clearly which parameters of the theory required modification. In particular, discrepancies have been noted between theory and experiment by as much as a factor of five for structures with thick, horizontal barriers, such as floors.

This discrepancy has been attributed by some investigators to the inadequacy of theory to account for radiation that is scattered in the vertical wall of a structure and attenuated by a horizontal barrier before reaching a detector location. This component of radiation, in the downward direction, such as in basement areas, is called "in-and-down" scattering and in the upward direction, through ceilings, is called "in-and-up" scattering.

An experimental evaluation of the attenuation afforded by horizontal barriers from both limited and infinite fields of contamination has been made. The experiment consisted of measuring the gamma-ray dose rates both below and above concrete floors in the three-story test structure located at the Protective Structures Development Center. The measure of attenuation in the downward direction was accomplished by collimating the detector below the floor barrier so that only radiation arriving from above was recorded. Attenuation in the upward direction was measured by reversing the collimation.

The primary purpose of the experiment was to obtain numerical values for horizontal barrier-reduction factors that could be compared with calculated values. Also, the horizontal barrier attenuation due to radiation originating from finite fields of ground contamination was investigated. Presently, there is no theory to account for this parameter.

The experiment was designed to measure the attenuation afforded by horizontal barriers both above and below ground to radiation that originated from sources lying on the ground surrounding a structure. Measured attenuation factors in the downward direction (in-and-down) agreed fairly well with calculated factors for the two-barrier mass thicknesses (48.6 and 97.2 psf) investigated.

The observed dose rates in the basement of the ceilingless structure agreed fairly well with the existing theory, while large discrepancies between theory and experiment were found in the experiment dealing with the structure basement which had a ceiling. This discrepancy increased with decreasing solid-angle fraction with the theory underestimating the dose rate in the basement by as much as a factor of three. The experimental results were consistent with past experiments conducted in basement structures in their comparison with theory. A modification to the theory in which a new barrier factor was calculated as a function of the barrier thickness and average solid-angle fraction subtended at the detector by the first-floor external wall agrees quite well with this experiment and past experimental results.

The calculated attenuation factors in the upward direction (in-and-up radiation component) underestimated the experimental results for large or infinite fields of contamination and overestimated the attenuation afforded by the floor from contamination within 50 feet of the structure walls.

ooo

PSDC-TR-25

A PRELIMINARY INVESTIGATION OF "IN-AND-DOWN" AND "IN-AND-UP" RADIATION COMPONENTS

By

J. VELLETRI

October 1966

Sponsored By

Office of Civil Defense
Office of the Secretary of the Army
Washington, D.C. 20310

Prepared By

CONESCO
A Division of Flow Corporation
Watertown, Massachusetts

Contract No. DA-18-020-ENG-3407
Work Order (OCD)-PS-65-17
Subtask 1117A

For the

PROTECTIVE STRUCTURES DEVELOPMENT CENTER
FORT BELVOIR, VIRGINIA
A BRANCH OF THE JOINT CIVIL DEFENSE SUPPORT GROUP
OFFICE OF THE CHIEF OF ENGINEERS
NAVAL FACILITIES ENGINEERING COMMAND
WASHINGTON, D.C.

SUMMARY

The technology of shelter calculation from fallout radiation has advanced in recent years, justifying confidence in protection factors computed for above-ground locations in simple, "box-type" structures exposed to an infinite field of ground contamination. For other situations, such as the basement of a structure or when a field of contamination is not infinite, either experimental data did not agree well with computed values or the experimental data, usually obtained from complex structures, failed to indicate clearly which parameters of the theory required modification. In particular, discrepancies have been noted between theory and experiment by as much as a factor of five for structures with thick, horizontal barriers, such as floors.

This discrepancy has been attributed by some investigators to the inadequacy of theory to account for radiation that is scattered in the vertical wall of a structure and attenuated by a horizontal barrier before reaching a detector location. This component of radiation, in the downward direction, such as in basement areas, is called "in-and-down" scattering and in the upward direction, through ceilings, is called "in-and-up" scattering.

An experimental evaluation of the attenuation afforded by horizontal barriers from both limited and infinite fields of contamination has been made. The experiment consisted of measuring the gamma-ray dose rates both below and above concrete floors in the three-story test structure located at the Protective Structures Development Center. The measure of attenuation in the downward direction was accomplished by collimating the detector below the floor barrier so that only radiation arriving from above was recorded. Attenuation in the upward direction was measured by reversing the collimation.

The primary purpose of the experiment was to obtain numerical values for horizontal barrier-reduction factors that could be compared with calculated values. Also, the horizontal barrier attenuation due to radiation originating from finite fields of ground contamination was investigated. Presently, there is no theory to account for this parameter.

The experiment was designed to measure the attenuation afforded by horizontal barriers both above and below ground to radiation that originated from sources lying on the ground surrounding a structure. Measured attenuation factors in the downward direction (in-and-down) agreed fairly well with calculated factors for the two-barrier mass thicknesses (48.6 and 97.2 psf) investigated.

The observed dose rates in the basement of the ceilingless structure agreed fairly well with the existing theory, while large discrepancies between theory and experiment were found in the experiment dealing with the structure basement which had a ceiling. This discrepancy increased with decreasing solid-angle fraction with the theory underestimating the dose rate in the basement by as much as a factor of three. The experimental results were consistent with past experiments conducted in basement structures in their comparison with theory. A modification to the theory in which a new barrier factor was calculated as a function of the barrier thickness and average solid-angle fraction subtended at the detector by the first-floor external wall agrees quite well with this experiment and past experimental results.

The calculated attenuation factors in the upward direction (in-and-up radiation component) underestimated the experimental results for large or infinite fields of contamination and overestimated the attenuation afforded by the floor from contamination within 50 feet of the structure walls.

FOREWORD

The experiments described in this report were performed during the period of August 1965-1966 by the CONESCO Division of Flow Corporation, Watertown, Massachusetts, at the Protective Structures Development Center, Fort Belvoir, Virginia.

This work was conducted for the Office of Civil Defense through the PSDC, Joint Civil Defense Support Group (JCDSG), Office of the Chief of Engineers, and was accomplished under Contract DA-18-020-ENG-3407, Work Order No. OCD-PS-65-17, Subtask 1117A.

Mr. R.F. Stellar is Chief of the JCDSG, and Mr. M.M. Dembo is Chief of its PSDC Division.

The author is indebted to Messrs. Charles McDonnell, Robert Spring, James Wagoner, and Steven Homa, of CONESCO, and Mr. G. Ploudre, of the PSDC staff, for their efforts in the performance of the experiments described in this report. Mr. C. Eisenhauer, of the National Bureau of Standards, and Mr. John Batter, of CONESCO, were helpful with their suggestions and criticisms.

TABLE OF CONTENTS

LIST OF ILLUSTRATIONS

LIST OF TABLES

NOMENCLATURE

$B_e(X_e, h)$	=	Attenuation introduced by a vertical wall to an infinite field of contamination
$B_{ws}(X_e, \omega_s)$	=	Attenuation introduced by a vertical wall to a finite field of contamination
$B'_o(X'_o)$	=	Attenuation introduced by a horizontal barrier to "in-and-down" scattered radiation
$B'_c(X_f, \bar{\omega})$	=	Modified values of the attenuation introduced by a horizontal barrier to "in-and-down" scattered radiation
$B_f(X_f)$	=	Attenuation introduced by a horizontal barrier to "in-and-up" scattered radiation
C_g	=	Ground contribution
D	=	Dose rate
D_o	=	Infinite field dose rate at three feet above a smooth plane
E	=	Eccentricity factor for the structure
$G_d(\omega, h)$	=	Cumulative angular distribution of direct radiation
$G_s(\omega)$	=	Cumulative angular distribution of scattered radiation
$G_a(\omega)$	=	Cumulative angular distribution of skyshine radiation
h, d	=	Detector height
H	=	Wall or story height
L(X)	=	Functional attenuation of the dose above an infinite field source covered with an attenuating mass of thickness X
$\ell(d, \cos\theta)$	=	Angular distribution of radiation in an air-over-ground infinite-field case
$S_a(d, \omega)$	=	Skyshine angular distribution
S'(X)	=	Skyshine attenuation function

NOMENCLATURE
(Continued)

$S_w(X_e)$	=	Fraction of radiation scattered by a vertical wall
$W(X,d)$	=	Attenuation introduced by a vertical wall normalized to 0.5
X_e	=	Vertical wall thickness in pounds per square foot (psf)
X_o	=	Basement ceiling thickness (psf)
X_f	=	Floor thickness (psf)
θ	=	Angle between an axis perpendicular to the plane of contamination and the direction of interest
ω	=	Solia-angle fraction (the solid angle divided by 2π)
$\bar{\omega}$	=	Average solid-angle fraction
ω_ℓ	=	Solid-angle fraction of the floor immediately below the detector
ω'_ℓ	=	Solid-angle fraction of the floor two floors below the detector
ω_u	=	Solid-angle fraction of the floor immediately above the detector
ω'_u	=	Solid-angle fraction of the floor two floors above the detector

1. BACKGROUND

Several methods for calculating the protection afforded by a structure against fallout radiation have been developed during the past few years. These methods were derived from basic data on radiation penetration developed by Dr. L. V. Spencer[1] in which the method of moments was used to determine solutions to certain idealized shielding configurations. Detailed procedures[2, 3] were developed by the Office of Civil Defense to calculate the protection afforded by existing buildings throughout the United States. The assumptions and the reasoning by which the calculations described in References 2 and 3 were derived from the basic data are discussed in detail in Reference 4.

Several experimental programs to evaluate these analytical procedures have been performed. In general, the calculations of reduction factors caused by ground sources of infinite extent are in good agreement with experimental results for "above-ground" single-story structures, the calculations being on the conservative side. This has not been the case for "below-ground" areas which receive a majority of their dose from radiation scattered from the atmosphere or structure above. Both full-scale[5, 6] and model[7] experiments have shown that the dose rate measured in basement areas was higher than that predicted, and its variation with depth was not expected from existing theory.[2, 3]

The problem of non-conservative dose-rate calculations for basement areas is of vital importance to the shelter analyst because of the large number of designated basement shelter areas. Recent investigations[8] modifying the present analytical methods of calculating dose rates in basement shelters have produced good relative agreement with experimental curves. Experiments conducted on multistory structures surrounded by ground sources of infinite extent have produced results that are in fairly good agreement with the calculated values (within about 20 percent) in above-ground areas, except for locations near the ceilings where the calculated values represent an underestimation of the dose.

Theoretical and experimental data on the dose contribution in below-ground areas from limited strips of contamination are meager. The only experimental evaluation that has been undertaken in this area was conducted on steel models. While the results of these experiments agreed fairly well with theory, the associated scaling problems in modeling prevented adequate validation of the theory. Recent experiments conducted at PSDC using circular limited strips of contamination have yielded results (reported here) as to the effects of the limited fields on the attenuation afforded by horizontal barriers to ground-based sources.

2. INTRODUCTION

The technology of shelter calculation from fallout radiation has advanced in recent years, justifying confidence in protection factors computed for above-ground locations in simple "box-type" structures exposed to an infinite field of ground contamination. For other situations, such as the basement of a structure or when a field of contamination is not infinite, either experimental data did not agree well with computed values or the experimental data, usually obtained from complex structures, failed to indicate clearly which parameters of the theory required modification. In particular, discrepancies have been noted between theory and experiment by as much as a factor of five for structures with thick horizontal barriers, such as floors.

This discrepancy has been attributed by Batter[8] to the inadequacy of theory to account for radiation that is scattered in the vertical wall of a structure and attenuated by a horizontal barrier before reaching a detector location. This component of radiation in the downward direction, such as in basement areas, is called "in-and-down" scattering and in the upward direction, through ceilings, is called "in-and-up" scattering. These components are described in detail in this report.

An experimental evaluation of the attenuation afforded by horizontal barriers from both limited and infinite fields of contamination has been made. The experiment consisted of measuring the gamma-ray dose rates both below and above concrete floors in the three-story test structure located at the Protective Structures Development Center. The measure of attenuation in the downward direction was accomplished by collimating the detector below the floor barrier so that only radiation arriving from above was recorded. Attenuation in the upward direction was measured by reversing the collimation.

The primary purpose of the experiment was to obtain numerical values for horizontal barrier-reduction factors that could be compared with calculated values. Also, the horizontal barrier attenuation due to radiation originating from finite fields of ground contamination was investigated. Presently, there is no theory to account for this parameter.

3. THEORY

3.1 GENERAL

In the analysis of structures with respect to shielding afforded from radioactive fallout, the level of radiation D at any point within structure is compared to

that of a standard position. The ratio D/D_o, called the reduction factor, is a measure of the effectiveness of that part of the structure against fallout radiation. D_o is taken as the specific dose rate three feet above an infinite smooth plane of contamination. This ratio, in general terms, is:

$$D/D_o = \left[\sum G(\omega, X_e) \right] \left[B(X_e, h) \right] \qquad (3.1)$$

where the left-bracketed term represents the attenuation caused by geometric effects and the right-bracketed term represents the attenuation caused by scattering and absorption in the barrier mass. The first term, that representing attenuation caused by geometry effects, is a function of the solid-angle fraction ω, subtended at the detector by the source, whether of primary or secondary nature, as well as the mass thickness X_e, interposed between source and detector. The barrier attenuation is a function of the mass thickness X_e of the barrier material, and the height, h, above the ground.

These concepts were extended into an engineering method[2] of shelter calculation. In this engineering method terminology, the reduction factor for ground-based sources of infinite extent becomes (Fig. 3.1 for schematic):

$$D/D_o = \left\{ \left[G_d(\omega_\ell, h) + G_a(\omega_U'') \right] \left[1 - S_w \right] + \left[G_s(\omega_U'') + G_s(\omega_\ell) \right] S_w E \right\} B_e(X_e, h) \qquad (3.2)$$

where $G_d(\omega)$ = "cumulative angular distribution" of direct radiation

$G_a(\omega)$ = "cumulative angular distribution" of atmospheric-scattered radiation

$G_s(\omega)$ = "cumulative angular distribution" of wall-scattered radiation

ω = solid-angle fraction (solid angle/2π)

S_w = fraction of emergent radiation scattered in wall barrier

E = eccentricity factor

h = detector height

$B_e(X_e, h)$ = barrier shielding introduced by a vertical wall of thickness X_e at height h above ground

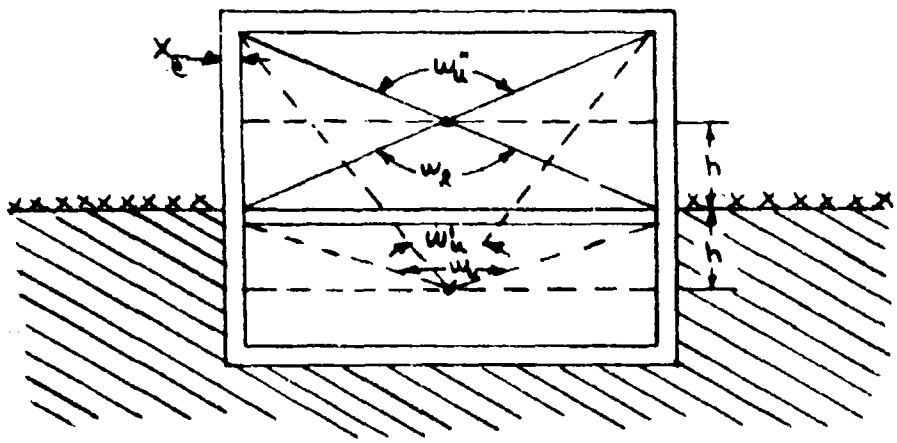

Single Story Structure with Basement

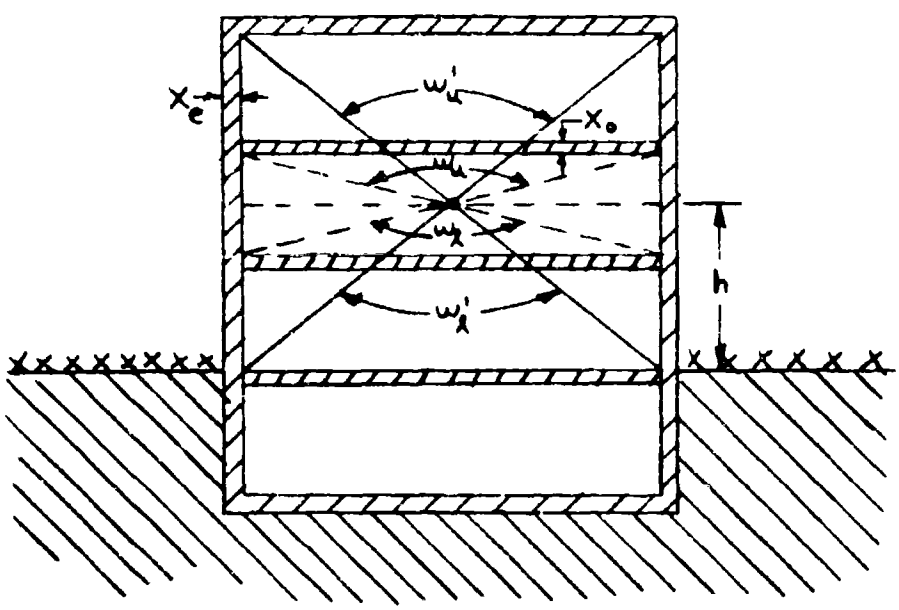

Multistory Structure

Application of Geometric Terminology of Engineering Manual

Figure 3.1

Although Equation (3.2) is basic to the engineering method[2] of calculating reduction factors in structures from a ground-based source of contamination, further refinements are required for structure variation from the simple box model. Common variations are basements, multistory structures, apertures, and interior partitions. Apertures and interior partitions were not involved in this experiment and thus are not discussed here in detail.

Radiation scattered to a basement area must undergo direct attenuation in the structure wall, be scattered in the direction of the basement, and then be attenuated by the basement ceiling. This mode of radiation penetration is called "in-and-down", and is expressed in terms of the presently-existing computational procedure as (Fig. 3.1):

$$D/D_o = \left\{ \left[G_a(\omega_U') - G_a(\omega_U) \right] \left[1-S_w \right] + \left[G_s(\omega_U') - G_s(\omega_U) \right] S_w E \right\} B_e(X_e, 3') B_o'(X_o') \tag{3.3}$$

where all terms are as previously defined and $B_o'(X_o')$ is the attenuation provided by the floor of the structure.

In computing the dose rate from ground-based sources of contamination in upper stories of a multistory structure, the contributions from the floor below and floor above the detector story are included in the total response of the detector. The general equation for computing the dose received by a detector located on the second floor of a three-story building (as shown in Fig. 3.1) is:

a. Second Story (detector floor)

$$C_{g1} = \left\{ \left[G_d(\omega_\ell', h) + G_a(\omega_U) \right] \left[1-S_w \right] + \left[G_s(\omega_U) + G_s(\omega_\ell) \right] S_w E \right\} B_e(X_e, h) \tag{3.4}$$

b. First Story (floor below detector)

$$C_{g2} = \left\{ \left[G_d(\omega_\ell', h) - G_d(\omega_\ell, h) \right] \left[1-S_w \right] + \left[G_s(\omega_\ell') - G_s(\omega_\ell) \right] S_w E \right\} B_e(X_e, h) B_f(X_f) \tag{3.5}$$

c. Third Story (floor above detector)

$$C_{g3} = \left\{ \left[G_a(\omega_U') - G_a(\omega_U) \right] \left[1-S_w \right] + \left[G_s(\omega_U') - G_s(\omega_U) \right] S_w E \right\} B_e(X_e, h) B_o'(X_o') \tag{3.6}$$

d. Total Dose (reduction factor)

$$D/D_o = C_{g1} + C_{g2} + C_{g3} \qquad (3.7)$$

The terms not previously defined are as follows:

C_g = ground contribution through a story of multistory structure

$B_f(X_f)$ = barrier factor for floor below detector

The above-ground shelter problem illustrated in Fig. 3.1 for the single-story structure is the most general case of the simple shelter situations. The overall approach to the multistory structure has been to break the ground contribution into three separate calculations. First, to consider the radiation penetrating the walls adjacent to the detector; that is, on the same floor; second, to consider the radiation which passes through the wall of the story above the detector; and third, to consider the radiation which penetrates the wall of the story below the detector. These same calculations could be continued for more stories above or below the detector, as required. Usually, however, it is only necessary to consider the stories immediately above and below the detector.

3.2 ACCURACY OF CALCULATED FUNCTIONS

Although estimates can be made of the accuracy of the functions used in the engineering method[2] of calculation in accordance with the precise situations upon which they are based, it is difficult to assess their accuracy in regard to the way in which they are commonly used to describe a real structure. In general, the barrier-reduction factors were calculated directly by Spencer[1], while in most cases, the geometry factors are estimates based upon the summation of angular distributions in various forms. Table 3.1 lists the function used in the engineering method; the basic function[1] and the estimated accuracy of this function in regard to the specific situation it is said to represent.

Ideally, a true evaluation of the parameters used in the functional equations for calculating shelter factors would result from measuring each of the parameters (especially the geometry terms) such that they may be evaluated discretely. Therefore, a combined approach of experimental and calculational evaluation has been undertaken.

TABLE 3.1

ACCURACY OF CALCULATED FUNCTIONS

OCD-PM-100-1 Function	NBS Function	Estimated[1] Accuracy (Percent)
$G_a(\omega)$	$S_a(d,\omega)$	0 to 25
$G_s(\omega)$	$S_a(d,\omega)$	0 to 25
$G_d(\omega)$	$(d,\cos\theta)$	0 to 25
$B_e(X_e,h)$	$W(X',d)$	10 to 25
$B'_o(X'_o)$	$S'(X)$	0 to 100
$B_f(X_f)$	$L(X)$	5

An experimental evaluation[9] of the vertical barrier factor $B_e(X_e,h)$ was recently conducted at the Protective Structures Development Center. The variation of the resultant attenuation up to a height of 33 feet above the contaminated plane was found to agree well with theory. Actual measured reduction factors were lower than those theoretically predicted by an amount equivalent to approximately 8 percent of the wall thickness. The calculated values of $B_e(X,h)$ presently used in shelter calculations are conservative by varying amounts ranging from 0 to 30 percent for wall thicknesses between 0 and 200 psf, respectively.

The horizontal barrier factors $B'_o(X'_o)$ and $B_f(X_f)$ or floor-shielding factors, as they are sometimes called, have little or no experimental verification. Discrepancies between theoretical and measured dose rates in basement areas have been attributed by some investigators[8] to the floor-attenuation function, $B_b(X'_o)$. This function stems from a basic calculation in which Spencer computed the detector response caused by radiation back-scattered (skyshine) to the detector from a plane source emitting gamma rays isotropically in an upward direction into an infinite homogeneous medium when the detector is below the source plane and separated by a mass thickness X (Fig. 3.2, a and b). He calls this function $S'(X)$, and estimates the error to increase roughly linearly with X from 0 percent at $S' = 1$ to as much as 100 percent at $S' = 10^{-4}$. The engineering method[2] of computations assumes that the angular distribution of radiation impinging on the basement ceiling from wall scatter resembles the

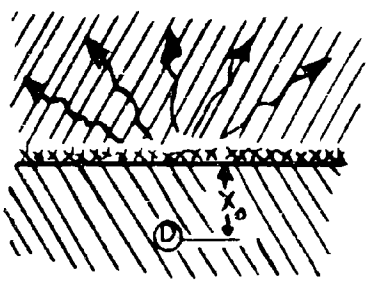

NBS - 42
S'(X)
(a)

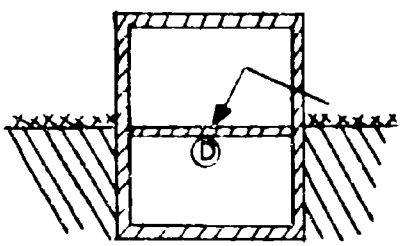

OCD- PM - 100 - 1
B'_o (X')
(b)

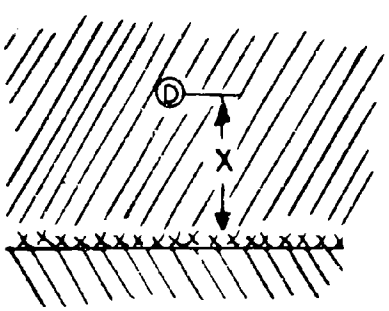

NBS - 42
L (X)
(c)

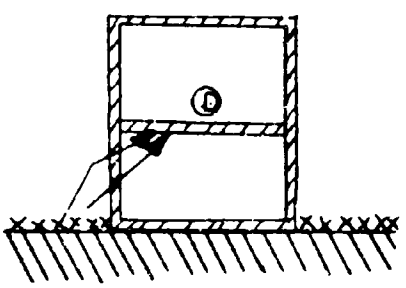

OCD - PM - 100 - 1
$B_f(X_f)$
(d)

Analytical and Physical Representation of Horizontal Barrier Reduction Factors

Figure 3.2

skyshine both in intensity and directional distribution and, therefore, the attenuation of the floor slab is taken as S'(X). The experiments described in this report were designed to measure this parameter.

The other aspect of the floor shielding considers the attenuation of radiation originating from below the detector. This radiation is composed of uncollided radiation from ground sources of contamination and radiation that is scattered by the wall of the story below the detector. The floor is assumed to attenuate these sources of radiation by a factor $B_f(X_f)$. This form of radiation attenuation is assumed to be similar to the total detector response from an infinite plane isotropic source separated by a mass thickness, X, in an infinite homogeneous medium. The estimated error in the basic function designated as L(X), as computed by Spencer, is five percent. The error introduced by how well the mathematical situation truly represents the physical situation may, of course, be much greater. This form of attenuation is illustrated in Fig. 3.2, c and d, as to the calculation model and physical representation as applied to engineering method[2] calculations.

4. EXPERIMENTAL ARRANGEMENT AND TECHNIQUE

4.1 GENERAL

The experiments described in this section were designed to measure the attenuation afforded ground contamination by horizontal barriers. The experiments attempted to duplicate physically the model of analysis used in the engineering method[2] and not the basic model from which the calculations were made by Spencer. The experimental technique consisted of constructing a collimator in a three-story concrete structure that would permit dose measurements from radiation sources above the detector plane (in-and-down), and of measurements from radiation below the detector plane (in-and-up).

Basic to the experiments were the tube-source technique and the radiation test structure, both of which have been discussed elsewhere[10]. However, since the test structure played such an important role in the experiment, its construction features will be considered in detail.

4.2 TEST STRUCTURE

The radiation test structure consists of a steel skeleton (Fig. 4.1) of internal dimensions 24 by 36 feet at the base, and 36 feet high, with provisions for

Photo of Assembled Building

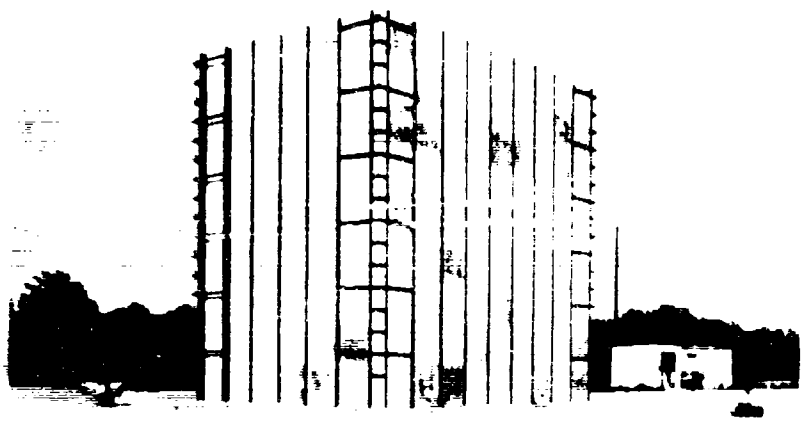

Photo of Skeleton of Building

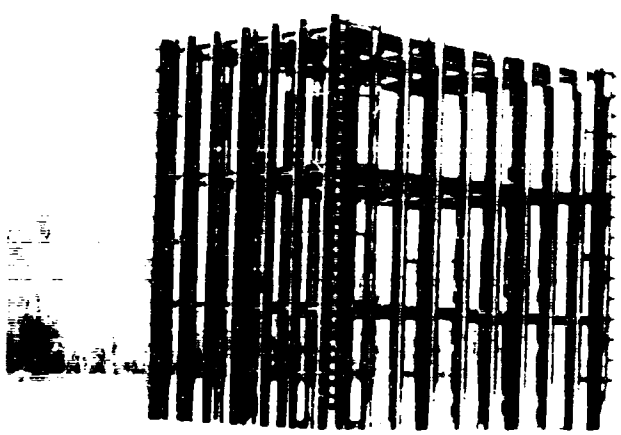

Figure 4.1 Test Structure at P. S. D. C. Radiation Test Facility

floors(or ceilings) at the 11-, 23-, and 35-foot elevations, and with a basement 6 feet in depth. The exterior building columns are 14B26 wide-flange beams which extend to the height of the building. A grid of 8-inch wide-flange beams spaced 4 feet on center and 12 feet on length stood at elevations of 11, 23, and 35 feet from the ground level (Fig. 4.1).

The structure can be made up to represent a variety of building configurations by assembling concrete panels (each 4 feet by 4 feet by 4 inches thick) into the desired modular design. The design allows floors and walls to be varied conveniently in thickness from 0 to 12 inches in 4-inch increments. Three combinations of wall and floor thicknesses were investigated in this experiment. The first was a 4-inch wall with 4-inch floors and roof; the second had 4-inch walls with 8-inch floors and roof, and the third had 8-inch walls and 8-inch floors and roof. The structure with 0 psf floors and 4-, 8-, and 12-inch walls was also investigated.

4.3 SIMULATED FALLOUT FIELD

The simulated field of contamination (the design of which is described in detail in Reference 10) consisted of a quadrant of a circle of 452-foot radius, concentric with the test structure, which was divided into four annular test areas (Fig. 4.2). Only one quadrant of the entire field had to be simulated, as the structure exhibited quarter symmetry; hence, the summation of dose rates of symmetrically-located detectors provided results equivalent to that which would have occurred if the full field had been simulated. The contaminated field was simulated by pumping sealed Cobalt-60 sources at constant velocity through a network of tubing that occupied each of four annular areas of the quadrant. The infinite field dose is the sum of the dosage received by the detector from each of the four areas, plus an estimated contribution based on the outermost simulated area to represent far-field sources of contamination. This estimate was based on the assumption that the attenuation of radiation caused by the structure arising from the farthest-out annulus was considered the same as that which would have occurred from contamination existing beyond the simulated areas. Since this generally represents less than approximately ten percent of the total dosage, the minor inaccuracy introduced by this assumption is usually negligible. This method of estimate is described in detail in Reference 10.

4.4 EXPERIMENTAL TECHNIQUE

The experimental technique consisted in measuring the radiation dose at points within the building from a simulated area of contamination of known

strength outside the building. Data were obtained using air-core-capacitor ionization chambers of 200-, 10-, or 1-mr capacity (dosimeters), together with a "charger reader" that functioned by measuring the total integrated current required to return a capacitor to its original voltage after exposure in the radiation field. Dosimeter (capacity) selection was based upon the exposure time, the section of the field being simulated, the thickness of the wall and floors, and the location of the test positions with respect to the contaminated area.

Prior to conducting this experiment, all dosimeters and the charger-reader were calibrated against a gamma source of known strength and National Bureau of Standards calibrated Victoreen R meters. All of the dosimeters selected for use in the experiment responded to within ±2 percent of the known dose. The chambers were also checked at intervals during the experiment using a secondary calibration procedure.

During this experiment, dosimeters were positioned in the basement at the center, at depths of 2, 3, 4, and 5 feet below ground level. Dose measurements were recorded at these positions for the four areas of contamination. The combination of wall and floor thicknesses investigated is presented in Table 4.1.

TABLE 4.1

EXPERIMENTAL WALL AND FLOOR COMBINATIONS INVESTIGATED

WALLS		FLOORS	
psf	Inches	psf	Inches
49	4	0	0
98	8	0	0
147	12	0	0
49	4	48.6	4
49	4	97.2	8
98	8	97.2	8

The mass thicknesses listed in Table 4.1 are for the concrete slabs only. In the experiments designated as 0 psf floors, a grid of 8-inch wide-flange beams

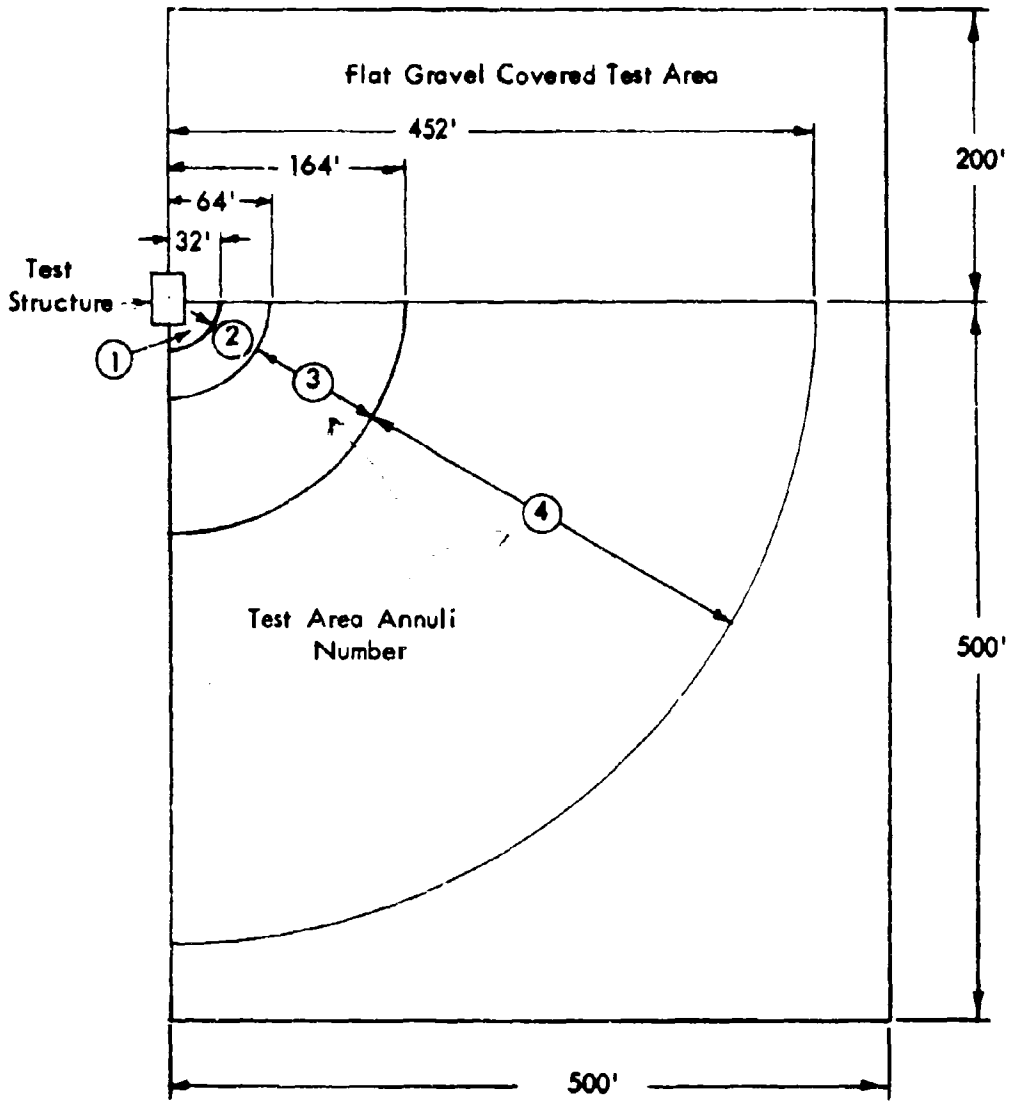

Plan View of Test Area

Figure 4.2

spaced 4 feet on center and 12 feet on length that support the concrete slabs existed. The dosimeter positions relative to the I-beams in the basement are illustrated in Fig. 4.3.

The attenuation afforded by the basement ceiling was measured by placing dosimeters directly above and below the concrete slabs that make up the ceiling. The dosimeter below was taped directly to the ceiling slab, and was shielded on all remaining sides with concrete block. This shielding configuration was designed to collimate the radiation, thus recording only that radiation penetrating the slab from above the detector plane. The dosimeter located above the ceiling at ground level recorded radiation that was deflected to the dosimeter after first scattering in the external vertical wall or air above the ceiling slabs. The ratio of the specific dose rates recorded in the shielded (below-slab) and unshielded (above-slab) positions is the attenuation afforded by the basement ceiling. Dose measurements were made in this manner for 4-inch (48.6 psf) and 8-inch (97.2 psf) ceiling slabs.

The technique used to measure the reduction in dose caused by floors above ground was essentially the same as that used in the below-ground experiment. Unlike the basement experiments in which only scattered radiation existed, the detectors above ground had to be shielded against both scattered and unscattered radiation. Preliminary investigation showed that the concrete blocks used in the basement ceiling experiment were not sufficient to collimate the lower dosimeter. Therefore, it was necessary to construct a lead-filled collimator for the "in-and-down" experiment above ground.

The collimator, as illustrated in Fig. 4.4, consisted of three main parts: wooden platform, core, and concrete blocks which surrounded the core. The core was made from a 30-inch-diameter, corrugated-metal pipe (14-gage steel) by filling the bottom three inches of its 20-inch height with concrete. The pipe was lined with concrete bricks and filled with lead shot. A concrete brick box was built on top of the lead and offset from the center and away from the radiation field (quarter symmetry used in the experiment). Access to the box was through a tunnel in the side of the pipe. This entrance, with the detector in place, was completely blocked with concrete bricks and bags of lead shot, as shown in Fig. 4.4. Concrete blocks in a double row completely surrounded the pipe so that a minimum of eight additional inches of concrete surrounded the outside of the core. This design, though cumbersome, was found necessary to reduce the "background" radiation to a point that meaningful measurements could be made. The reduction in dose rate afforded by this combination of concrete and lead was calculated to be about 1.63×10^{-6}. Because of the weight and size of the collimator, only one above-ground floor was investigated.

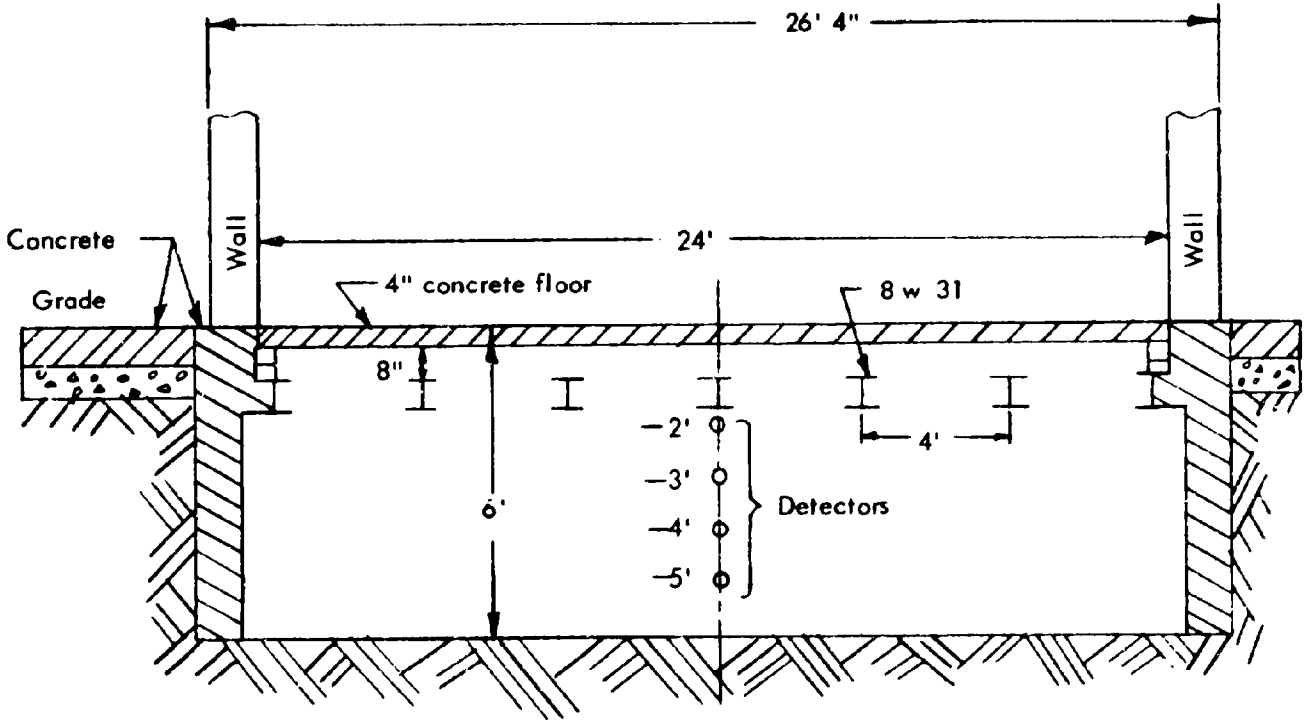

Basement of Test Structure at P. S. D. C.

Figure 4.3

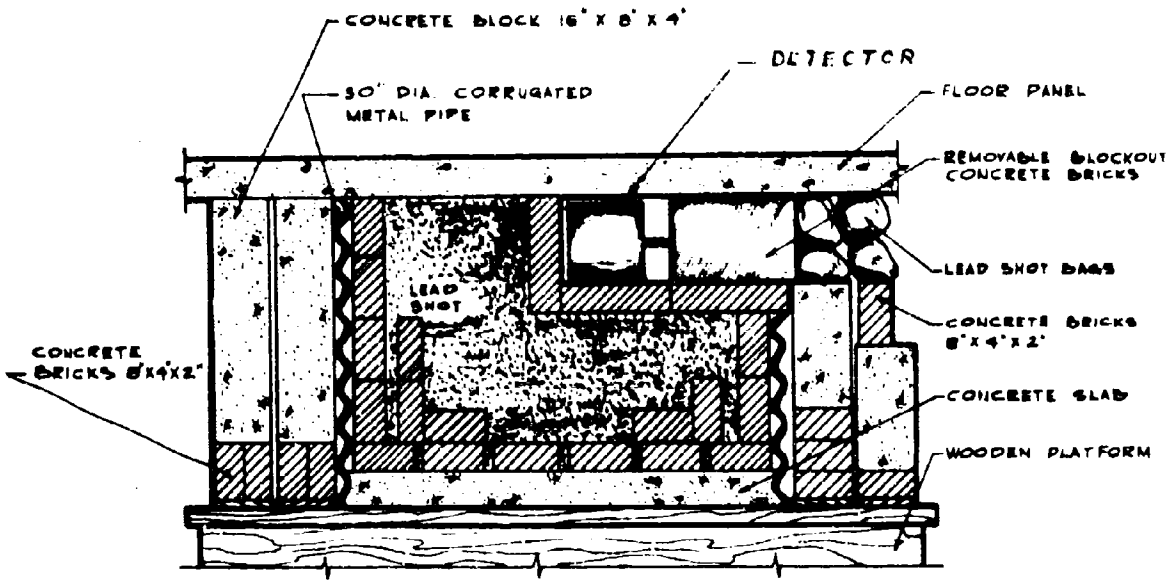

SECTION A-A

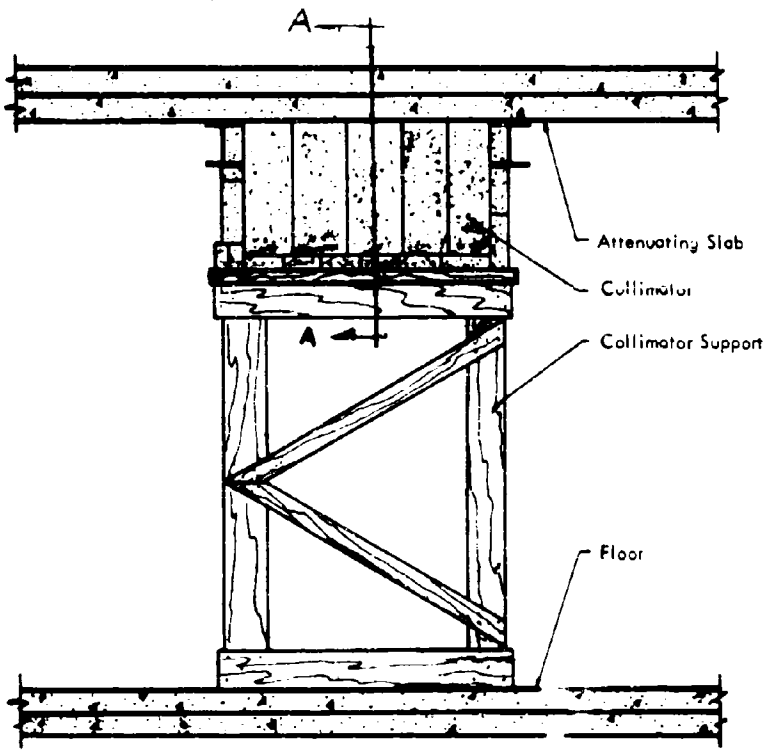

Collimator Type Shield for Detector

Figure 4.4

The "in-and-up" measurements were made with the collimation reversed. The detector attached to the ceiling was unshielded, while the detector directly above the floor was shielded. Concrete blocks were used to shield the detector above the floor. The amount of shielding required for this experiment was considerably less than that used in the "in-and-down" experiment, because only scattered radiation was involved.

4.5 NORMALIZATION AND ACCURACY OF EXPERIMENTAL DATA

All dosimeter readings were normalized to a specific dose rate; that is, to a per-hour basis for an equivalent contamination density of 1 curie of Co-60 per square foot (1 curie Co-60 = 14r/hr at 1 foot at STP). This is the source density that produced a radiation field of 464 r/hr three feet above an infinite, smooth, uniformly-contaminated plane in an earlier experiment[10] conducted at this facility. Dosimeter readings were converted to an r/hr basis, using dosimeter-calibration constants, exposure time, source strength, and temperature-pressure corrections for the effect of atmospheric conditions. The normalization is described in detail in Reference 10. Data tables for this experiment are presented in Appendix A.

To determine the accuracy of the data obtained from these experiments, the errors or uncertainties of many parameters must be considered. Since it was impractical to determine experimentally, in a completely vigorous way, all of the uncertainties associated with weather, exposure time, source strength, and so forth, it was necessary to estimate some of the errors and uncertainties from practical experience. A detailed analysis of those errors is presented in Appendix B. By compounding these values according to accepted principles, the estimated percentage of standard deviation in the specific dose rate and infinite field reduction factor is three and four percent, respectively.

5. RESULTS AND ANALYSIS

5.1 GENERAL

For convenience in presentation and discussion, the results of this experiment have been separated into two main parts; (1) data taken below ground (basement), and (2) data taken above ground. The below-ground data are analyzed in terms of reduction factors in the basement, and attenuation afforded by the horizontal barrier (ceiling). The above-ground data are evaluated in terms of floor-attenuation factors from both "in-and-up" and "in-and-down" scattered radiation.

5.2 BELOW-GROUND DATA

5.2.1 Basement Without Ceiling - Experimental data in the form of reduction factors are presented in Table 5.1 as a function of a detector depth below ground and solid-angle fraction for all the combinations of wall and floor thicknesses investigated. These values are compared with theoretical values in Fig. 5.1 and Fig. 5.2. The theoretical values shown in these figures were calculated using the engineering method[2] (Equation (3.3) of this report) and Co-60 functions from NBS-42[1]. Fig. 5.1 shows the dose distribution in the center of the test structure basement for three wall thicknesses without a concrete floor. The relative agreement, i.e., curve shape, as shown on this figure is quite good for the three wall thicknesses tested, while the calculated values are almost a factor of two higher in all cases. Part of this discrepancy in absolute values can be attributed to the attenuation provided by the grid of 8-inch wide-flange beams that are permanently fixed in the test structure and which is not accounted for in the calculational procedure. This discrepancy in terms of mass thickness is approximately equal to the calculated attenuation afforded by a 5-psf floor. This is illustrated in Fig. 5.2, in which the experimental results are compared with calculated values, assuming $B'_0(X'_0) = 0.54$ in Equation (3.3), where X_0 is equal to 5 psf. (Note: If the steel were uniformly smeared over the area, it would represent approximately 9.6 psf equivalent thickness). It should be noted here that the calculated horizontal barrier factor $B'_0(X_0)$ is extremely sensitive to slight changes in barrier mass thickness because of the steep slope of the curve, particularly near zero mass (for example, see Figure B-17 of Reference 1).

5.2.2 Basement With Ceiling - Experimental reduction factors in the basement of the structure with 4- and 8-inch concrete ceilings are compared with theoretical values in Fig. 5.3. It is evident that the experimental curve does not follow the calculated curve, and the slopes of the experimental curves with and without concrete ceilings are not the same. While the flattening of the dose curve in basements near the ceiling has been observed in most previous experiments, it is more pronounced in this experiment because of the effect of the steel beams. The effect of this additional mass on dosimeter locations directly below the beam (2- and 3-foot depths) is illustrated in Fig. 5.4. Here the measured values in the center of the basement directly beneath the center beam (see Fig. 4.3) are compared with values measured at an offset distance of 2 feet from the center. The 2- and 3-foot detector positions in the center are 4 inches and 1 foot, 4 inches, respectively, below the steel beam. The increase in dose rate as the detectors are offset 2 feet from the beam is 63 and 10 percent of the 2- and 3-foot depths, respectively, while the 4- and 5-foot depths show excellent agreement, as expected. It is evident from this plot that

TABLE 5.1

EXPERIMENTAL REDUCTION FACTORS TEST STRUCTURE BASEMENT

(Center Line/Infinite Field)

		Reduction Factors					
H (Ft)	Solid-Angle Fraction ω	4" Walls 0 Floor	8" Walls 0 Floor	12" Walls 0 Floor	4" Walls 4" Floors	4" Walls 8" Floors	8" Walls 8" Floors
-2.0	0.87	0.037	0.014	0.0049	0.0013	0.00016	0.000068
-3.0	0.81	0.029	0.011	0.0037	0.0017	0.00021	0.000089
-3.5	0.78	0.027	0.0098	0.0036			
-4.0	0.75	0.025	0.0096	0.0033	0.0018	0.00028	0.00010
-5.0	0.70	0.023	0.0087	0.0030	0.0018	0.00026	0.00014

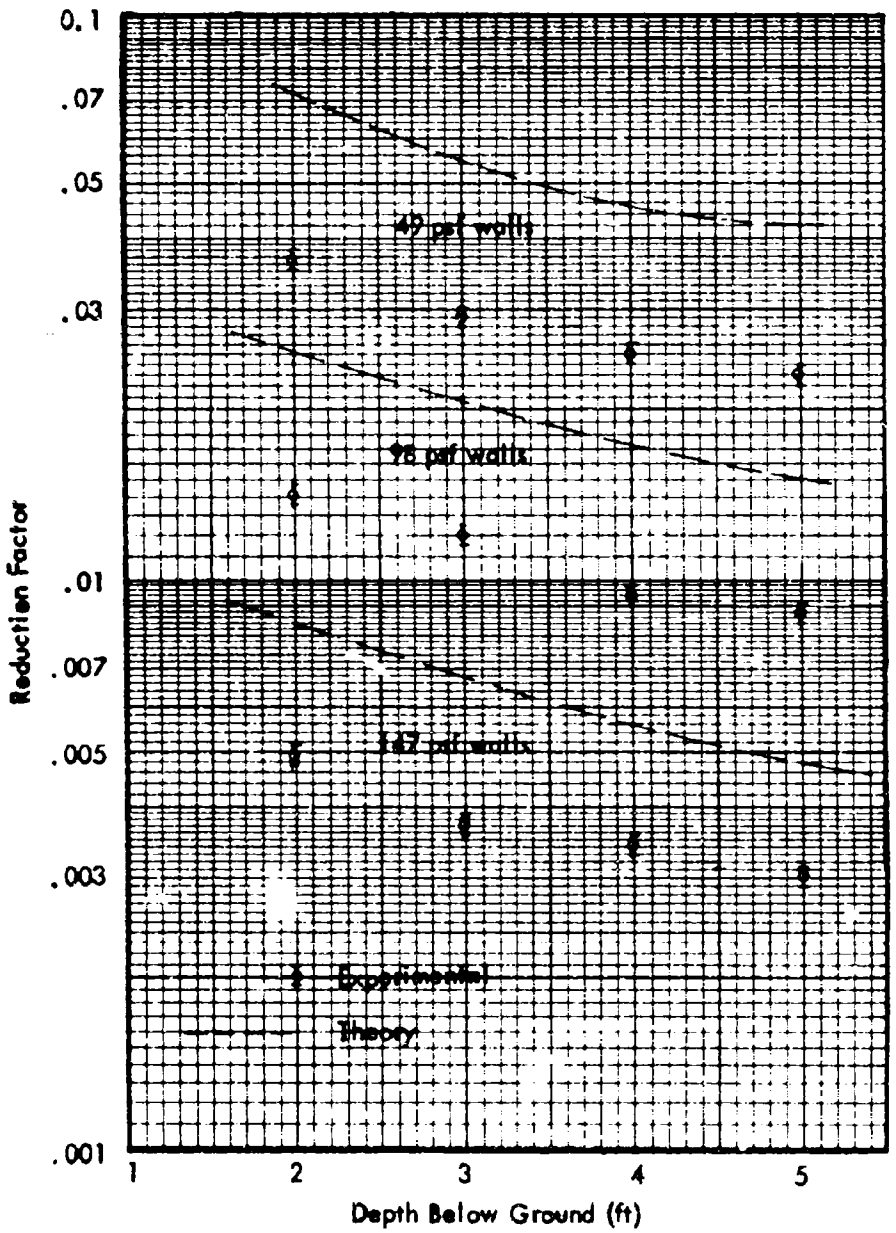

Infinite Field Reduction Factor in Test Structure Basement
With No Floors

Figure 5.1

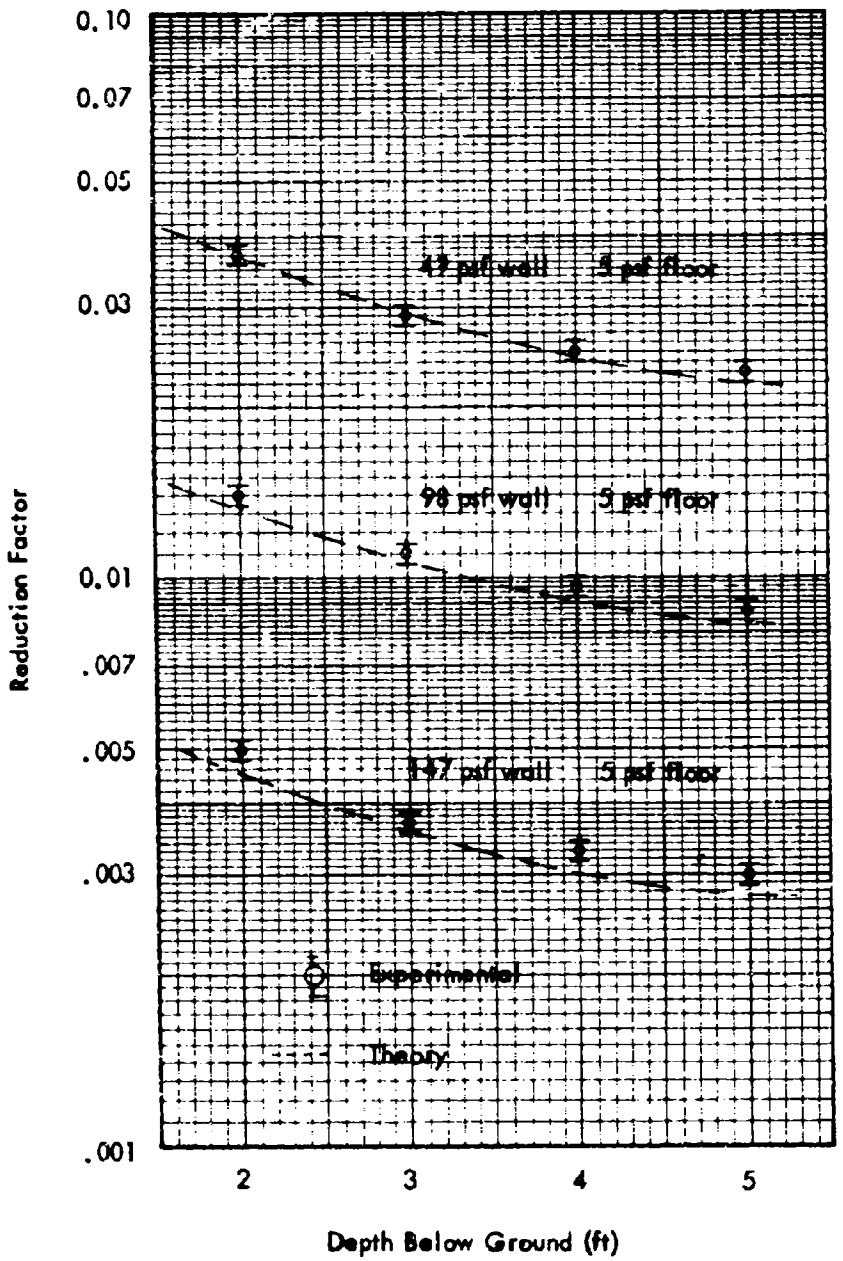

Infinite Field Reduction Factor in Test Structure Basement
(Estimated Effects of Steel Beams Included)

Figure 5.2

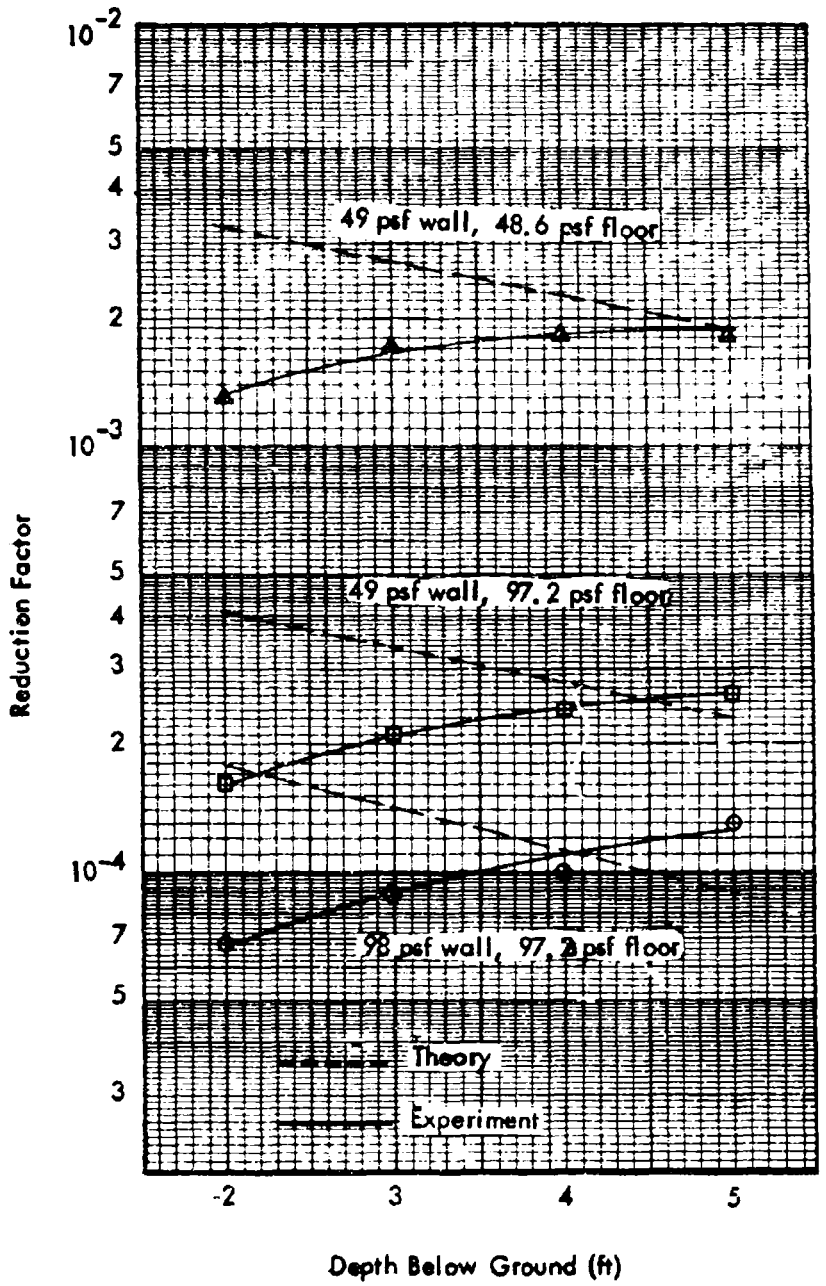

Comparison of Experimental and Theoretical Reduction Factors
Neglecting the Effect of the Steel Support Beams

Figure 5.3

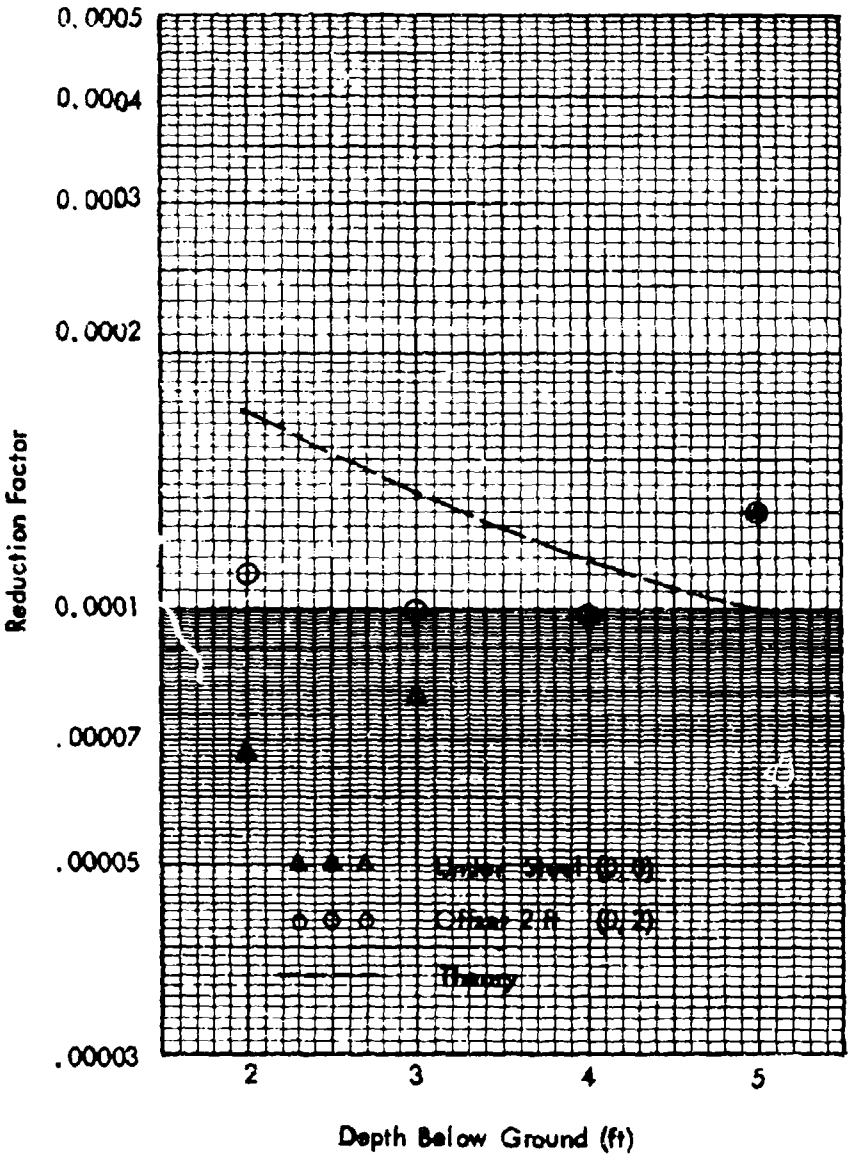

Comparison of Center and Off Center Dose Rates in the Basement (98 psf Walls and 97.2 Floors)

Figure 5.4

the steel beams produce local perturbations in the experimental curve which cannot be accounted for with present calculational methods. The calculated curve presented in Fig. 5.4 does not include any allowance for the attenuation introduced by these beams and, hence, is shown for comparison only.

The experimental results for the three building configurations with basement ceilings are compared with theoretical values in Fig. 5.5. The dashed lines are calculated values with an additional 5-psf steel attenuation factor as determined from the open-basement experiment. The solid lines are calculated values for an added 9.6-psf steel attenuation factor, which represents attenuation afforded by the beams if they were smeared and occupied the complete ceiling area. If the current methods of calculations were correct, the combined attenuation afforded by the concrete slabs and steel beams should fall somewhere between the two curves.

5.2.3 Comparison With Previous Work - The results of this experiment can be compared with a recent experiment[11] conducted at the Nuclear Defense Laboratory, Edgewood Arsenal, Maryland, and experiments reported in Reference 5. Experimental reduction factors as a function of solid-angle fraction are shown in Fig. 5.6 for basements with and without ceilings. Because the wall and ceiling thicknesses were different in the three experiments, a direct numerical comparison cannot be made. However, the experimental curves shown on this figure are representative of dose distributions observed in basement areas by many investigators[5,8,11]. The agreement between NDL and this experiment as to the slope of the curve in an open basement (no ceiling case) is good. Also, the slopes of the curves for the basement with ceilings agree, with the exception of the PSDC experiment, where the steel beams affected the dose rates at the higher solid-angle fractions (ω = 0.81 and 0.87). It is evident from Fig. 5.6 that the ceiling attenuation depends on position, as well as barrier thickness, whereas the calculations assume no dependence on position. This is illustrated in Fig. 5.7, in which experimentally-measured reduction factors from these experiments are compared with calculated values as a function of solid-angle fractions. Note that the calculated values shown for the basement of Reference 5 do not include the attenuation afforded by the concrete beams that supported the ceiling. The data of Reference 11 presented in Fig. 5.7 was taken on a structure containing no roof. Thus, skyshine through the "roof" and ceiling shine is not accounted for properly in the standard computational method[2]. A minor modification suggested by LeDoux[13], however, separates the skyshine-ceiling shine component so that it may be properly analyzed. This equation,

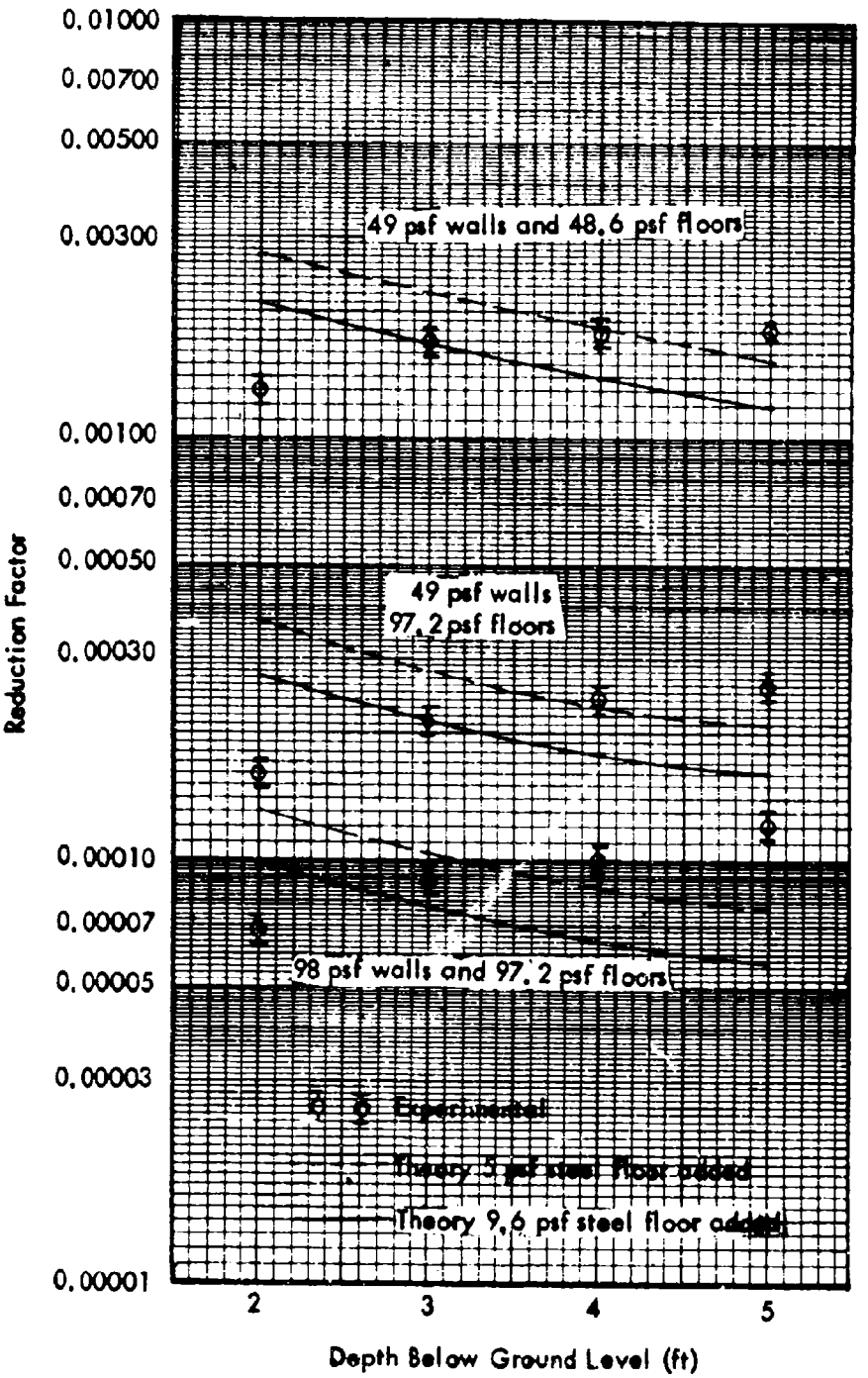

Comparison of Experimental and Theoretical Reduction Factors
in a Basement Area
(Theory Includes Steel Effect)

Figure 5.5

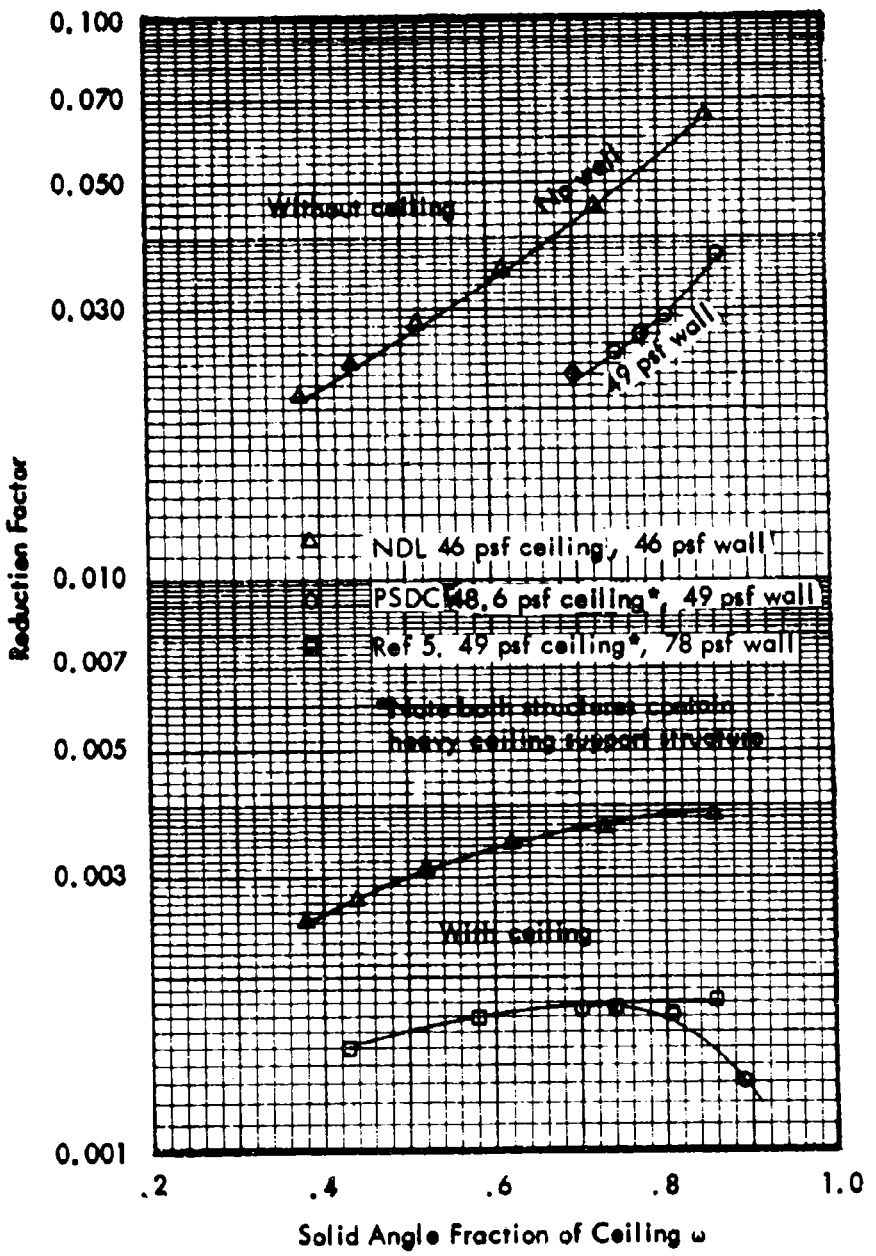

Comparison of Experimental Reduction Factors
With and Without Ceiling in Place

Figure 5.6

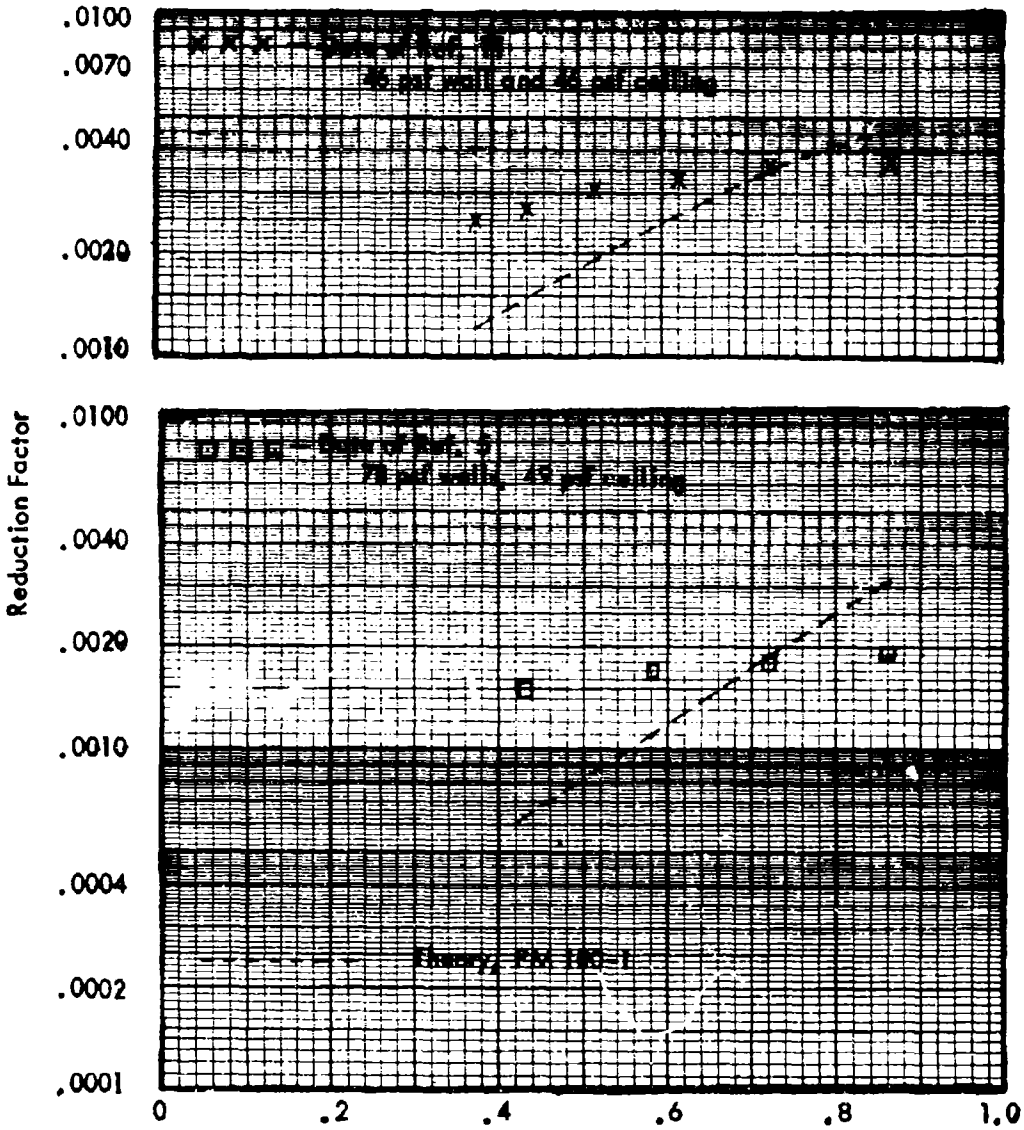

Comparison of Calculated and Experimental
Reduction Factors for Two Previous Basement Experiments

Figure 5.7

$$D/D_o = B'_o(X'_o)\left[B_e(X_e,h)\ S_w E\left[\left|G_s(\omega'_U) - G_s(\omega_U)\right| + B_e(X_e,h)\ (1-S_w)\right.\right.$$
$$\left.\left.\left|G_U(\omega'_U) - G_U(\omega_U)\right| + B'_o(X_c)\left|G_U(\omega=o) - G_U(\omega'_U)\right|\right]\right] \quad (5.1)$$

where $G_U(\omega_U)$ = The directional response for non-wall-scattered radiation from above the detector plane, not including ceiling shine

$B'_o(X_c)$ = Ceiling attenuation factor ---- equal to unity when no ceiling is present

then allows the computation of the dose to be expected in the building of Reference 11. The significant feature of the curves shown in Fig. 5.7, as in the PSDC experiment shown on Fig. 5.5, is the difference in the slope of the experimental and calculated curves.

The experimental curves are seen to be much flatter than the calculated curves; i.e., the decrease in observed dose is not as great as the decrease in calculated dose as the detector is moved away from the ceiling (decreasing solid-angle fraction). Also, reasonable agreement is achieved at the higher solid-angle fractions (near ceiling). This was expected, because the ceiling barrier factor $B'_o(X'_o)$, as calculated by Spencer, was for a detector directly on the ceiling.

The horizontal barrier factor $B'_o(X'_o)$ was experimentally determined for two ceiling mass thicknesses in the PSDC test structure basement. The experimental technique and arrangement are described in Section 4.3 of this report. Experimentally measured barrier factors are shown in Fig. 5.8 as a function of radius of contamination. Values calculated for the two mass thicknesses tested are also shown for comparison. It should be noted that while the experimental values shown are for limited strips of contamination and summed to determine the infinite field value, only infinite-field calculated values are available.

Agreement between calculated and experimental barrier factors for large or infinite fields of contamination is within 25 percent, with the calculated value underestimating the attenuation afforded by the ceiling. For close-in contamination, the calculated values represent an underestimation of the attenuation afforded by the ceiling by as much as 50 percent. Unlike the experiments conducted to determine the depth-dose variation in the basement, the steel beams had little or no effect on the values measured in this experiment, because only

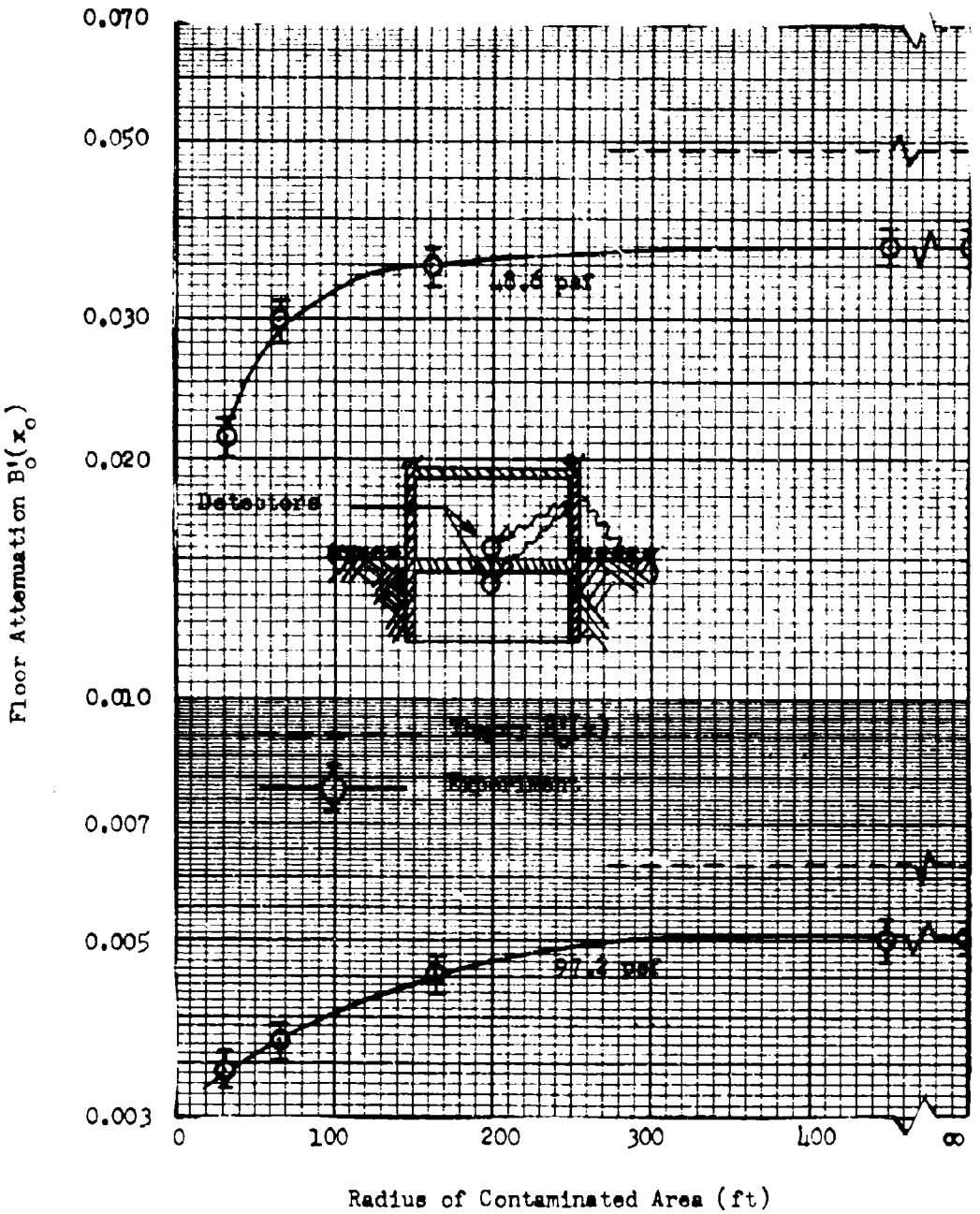

Floor Attenuation as a Function of the Radius of the Contaminated Areas Surrounding the Structure

Figure 5.8

radiation incident and penetrating the ceiling slab within a few inches of the detector was considered. The nearest steel support beam to the detector was approximately two feet away.

It is of interest to compare experimentally-measured and calculated reduction factors for the two locations in this experiment. These values are shown in Fig. 5.9 as a function of radius of contamination. The experimental reduction factors were determined by dividing the specific dose rate, measured at the detector position for a finite field of contamination, by the infinite field specific dose rate three feet above a uniformly-contaminated plane. The theoretical values shown on Fig. 5.9 were calculated using the engineering method[2] of limited strips of contamination. Briefly, this method consists of accounting for the finite contaminated area by substituting a limited-strip barrier factor $B_{ws}(X_e, \omega_s)$ into Equation (3.2) for the infinite field barrier factor $B_e(X_e, h)$. As can be seen from this figure, the relative agreement between calculated and experimental values is quite good for both position A (above) and position B (below) the ceiling slab. The calculated values are conservative, or represent an overestimation of the dose arriving at the two positions.

In summary, the relative agreement between calculated and experimental reduction factors in an open basement (no ceiling) is quite good, with the calculated values overestimating the dose received in the basement. When a basement ceiling is added, the calculated reduction factor curves do not agree well with experimental reduction factor curves, and can represent an underestimation of the dose received in the basement by as much as a factor of three, or more. The discrepancy between theory and experiment increases with decreasing solid-angle fractions, with agreement near the ceiling (solid-angle fraction greater than 0.7) quite good.

The discrepancy between theory and experiments in dose distribution in a basement may be caused by any one, or a combination, of the variables in Equation (3.2). The only variable that is a direct function of the ceiling thickness is $B'_o(X'_o)$. As the calculated reduction factors near the ceiling agree quite well with experimental values, and disturbing discrepancies are noted at the lower solid angles, it appears that $B'_o(X'_o)$ should also include a geometric effect that is not accounted for in Equation (3.2).

5.2.4 Modification to Existing Theory - A recent study[8] on "in-and-down" scattered radiation attributes the discrepancy between theory and experiment to the calculated attenuation values used for the ceiling slab over the basement. Batter[12] has estimated the expected attenuation of a ceiling

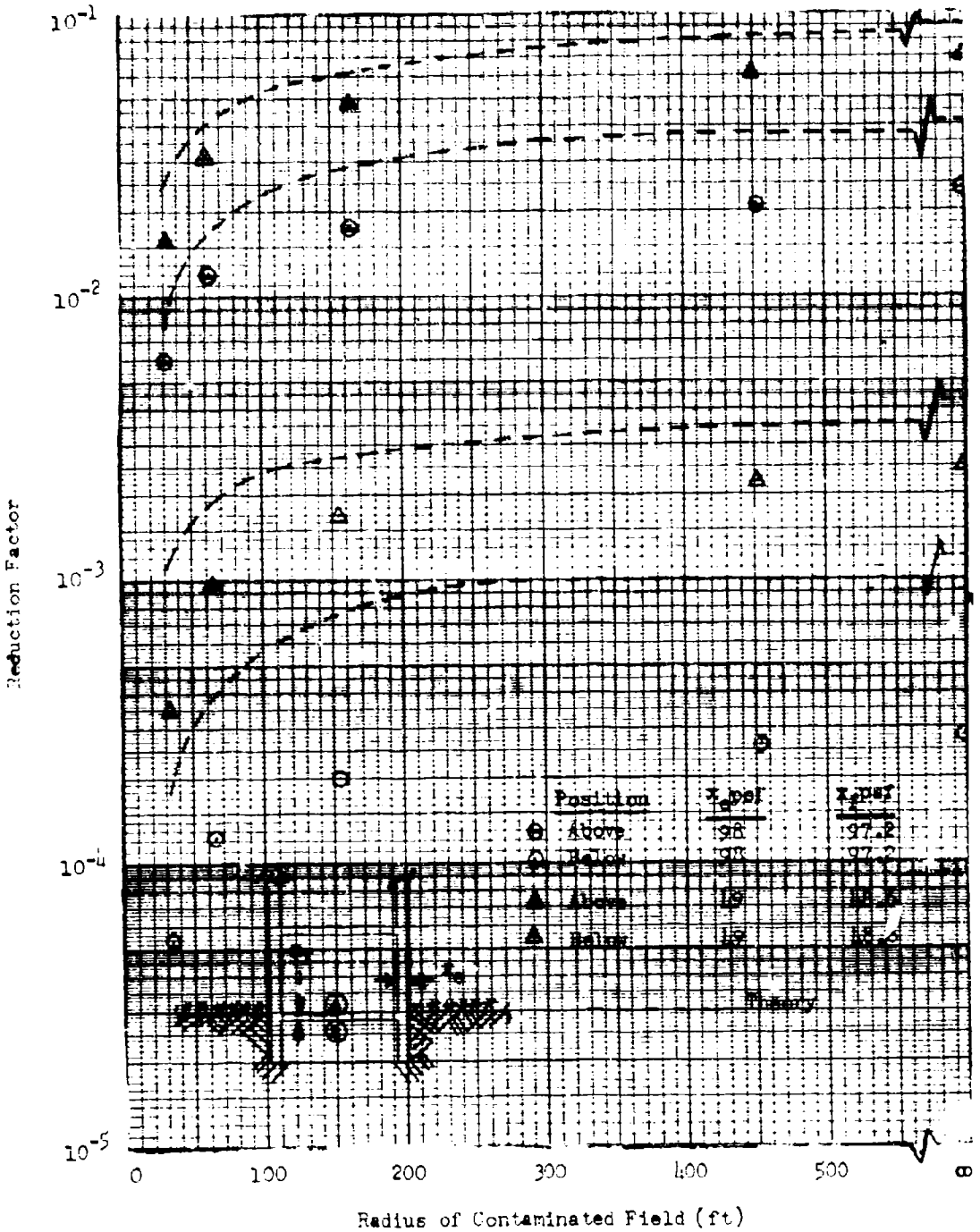

Calculated and Experimental Reduction Factors for Positions Above and Below the Basement Ceiling

Figure 5.9

slab by assuming Compton first-collision scattering in the exterior walls and attenuation coefficients computed for parallel slant-incidence photons. He calculated this attenuation in approximate form, based upon the 3-foot angular distribution of impinging radiation. Thus, a new function $B'_o(X,\bar{\omega})$, where X is the mass thickness of the ceiling slab and $\bar{\omega}$ is the average solid-angle fraction (see sketch in Fig. 5.10) from the vertical wall to the detector, has been created. Curves of this parameter as a function of mass thickness and average solid-angle fraction are reproduced in Fig. 5.10. This computation contained several conservative assumptions, and the author has recommended that the attenuation values computed by this method be increased by about 20 percent for ceiling thicknesses greater than about 20 psf.

The results from this experiment can be expressed in the form of barrier attenuation as a function of solid-angle fraction by taking the ratio of the experimental reduction factors with and without a basement ceiling. These values are shown in Fig. 5.11 for 97.2 and 48.6 psf barriers as a function of the average solid-angle fraction $\bar{\omega}$. The relative agreement of the slopes between the new function calculated by Batter and the experimental results as a function of solid-angle fraction is good, with the function $B'_o(X_f,\bar{\omega})$ underestimating the attenuation afforded by the barriers by about 50 percent. The discrepancy in absolute values for the PSDC experiment can partly be attributed to the uncertainty of the effective mass thicknesses of the ceiling barrier used in the experiments (because of the steel beams that supported the concrete slabs). The effective mass thicknesses used in Batter's function was for the concrete slabs only. Therefore, while a true absolute comparison cannot be made, allowance for the extra mass provided by the steel beams in the function $B'_o(X,\bar{\omega})$ would produce closer agreement. The function $B'_o(X'_o)$ appears as a straight line on this graph, because it is a function of the barrier mass thickness only, and is shown for comparison. It is evident from the comparison on Fig. 5.11 that the modified function $B'_o(X,\bar{\omega})$ is in better agreement with the experiment than the function $B'_o(X'_o)$ presently used in calculated procedures.

This is also illustrated in Fig. 5.12. Here theoretical reduction factors were calculated substituting the function $B'_o(X,\bar{\omega})$ for $B'_o(X'_o)$. These factors are compared with the experimental data of References 5 and 11. The calculated reduction factors based on the new function are again conservative and agree fairly well with the experimental results in both basements.

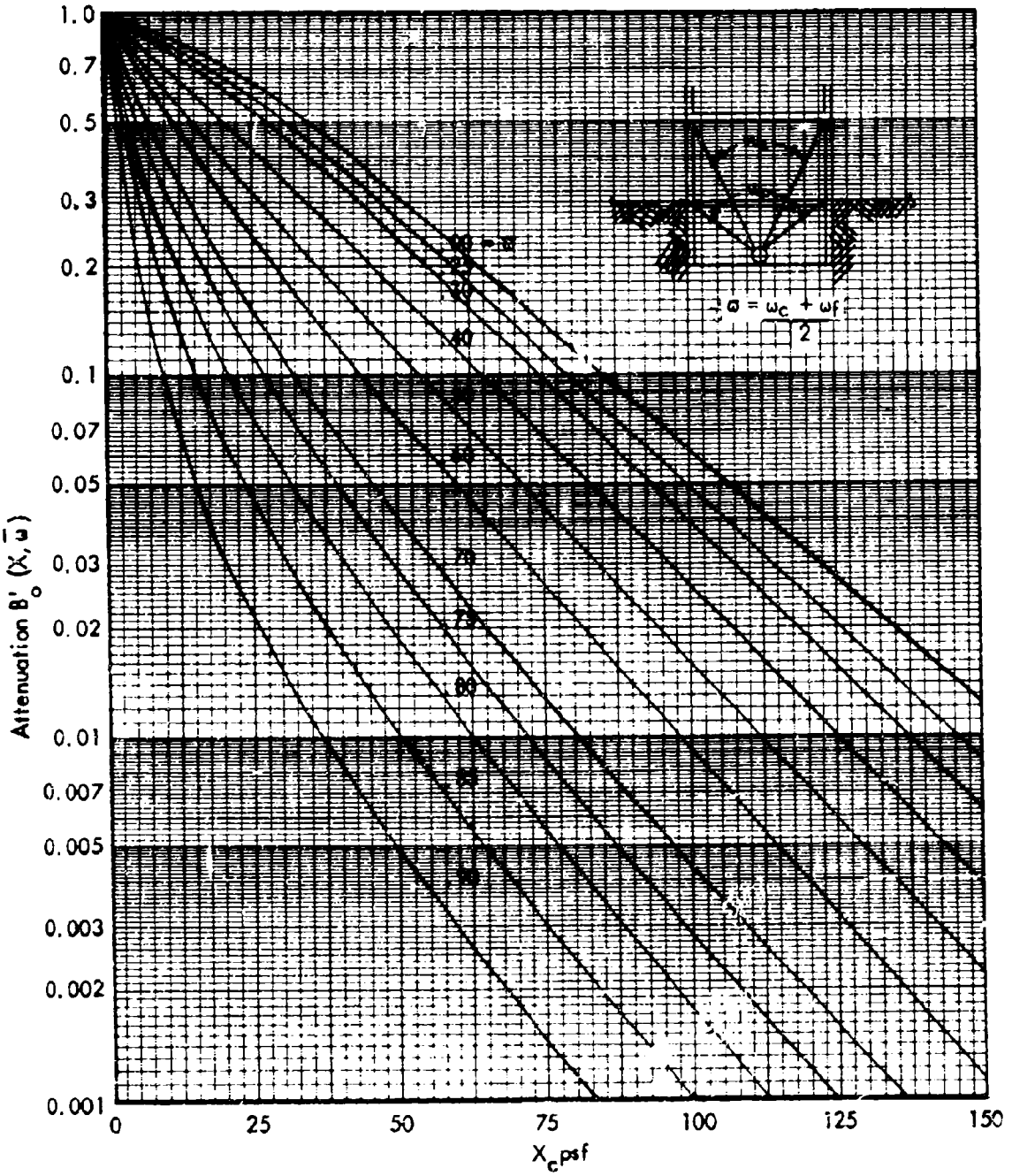

Floor Attenuation, 1.25 mev - from Batter[12]

Figure 5.10

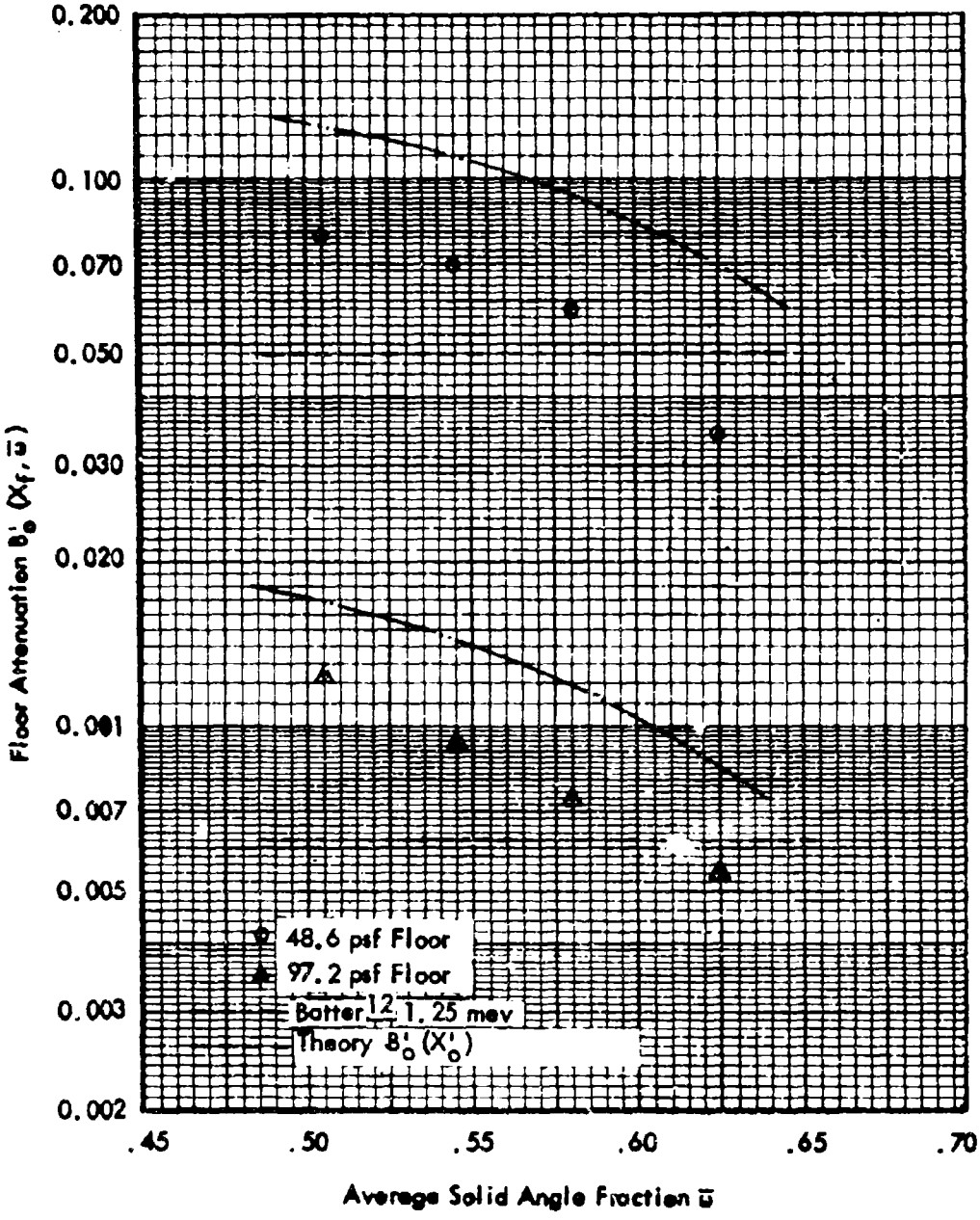

Comparison of PSDC Experimental Floor Barrier Factor
With Batter's Modified Barrier Function $B'_o(X_o \bar{\omega})$

Figure 5.11

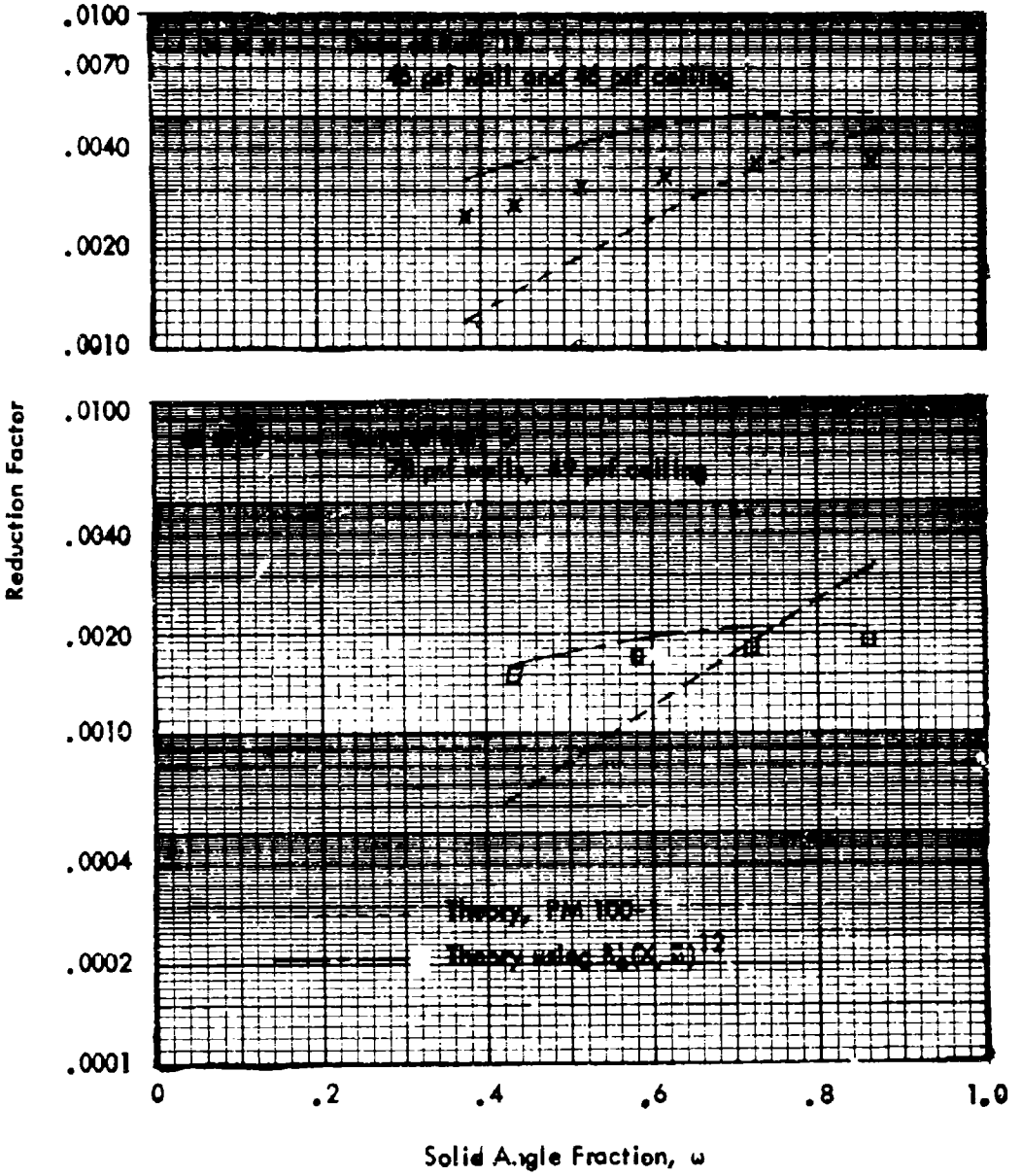

Comparison of Two Previous Basement Experimental Reduction Factors With Calculated Reduction Factors Using the New Function $B_0'(X, \Omega)$

Figure 5.12

5.3 ABOVE-GROUND DATA

5.3.1 "In-And-Down" Radiation Component Above Ground - The attenuation afforded by a ceiling from radiation that was scattered in the wall or air above the detector was measured for two ceiling mass thicknesses. As was previously stated in Section 4.3, Experimental Technique, this experiment required the use of a large collimator, composed of a concrete block and lead shot, to shield against the non-scattered radiation now visible to the detector from the ground contamination. Preliminary experimentation on the structure with 4-inch floors indicated the need for such a massive collimator. Because of the weight and size of the collimator, only one above-ground floor was investigated. The results of this experiment for the four areas of contamination are presented in Table 5.2, together with the background dose rates with both detectors shielded. It should be noted here that the estimated experimental errors, as discussed in Section 4.5 and Appendix B, are based on mid-scale instrument readings. Because of the limitation in instrumentation and sources, it was necessary to accept some low-scale readings in the shielded positions of this experiment which could produce somewhat higher experimental errors.

The results from this experiment are shown in Fig. 5.13 in the form of floor-shielding factors $B_0'(X_0')$ as a function of radius of contamination. The lower solid curve shows the experimental floor-shielding factor as a function of radius of contamination with the background radiation subtracted from the shielded detector, while the upper solid curve includes background. The discrepancy between the two curves within a radius of contamination of 100 feet can be attributed to the inadequacy of the collimator to shield against close-in sources. It is believed that the bottom curve is more representative of the floor-barrier reduction as a function of contaminated radius.

The theoretical function $B_0'(X_0')$ is shown on Fig. 5.13 as a dashed curve. Note that the theoretical function appears as a straight line on this graph because it was calculated for an infinite field of contamination, but since it is used also in the calculations for limited fields of contamination, the comparison is of interest. The theoretical function can be seen to be conservative by as much as a factor of two for close-in contamination; i.e., the calculated function underestimates the attenuation afforded by the floor barrier.

5.3.2 "In-And-Up" Radiation Component - The "in-and-up" radiation floor-barrier factor was measured for two floor thicknesses. These values, in terms of specific dose rates above and below the floor barrier, are presented in Table 5.3 as a function of the radius of contamination from the center of

TABLE 5.2

Experimental Results of "In-And-Down" Radiation Component

(Second Story of Multistory Test Structure with 97.2 psf Floors)

$D = (r/hr)/(curie/ft^2)$

Area	Above Floor	Below Floor (Shielded Below)	Background
	D_A	D_B	
I	.181	.001	.00077
II	.94	.0035	.0012
iII	1.64	.0072	.00074
IV	1.45	.0060	.0015

Radius of Contamination (ft)	D_B/D_A	$\frac{D_B - \text{Background}}{D_A}$
0 to 32	.0055	.0011
0 to 64	.0040	.0022
0 to 164	.0042	.0033
0 to 452	.0042	.0033

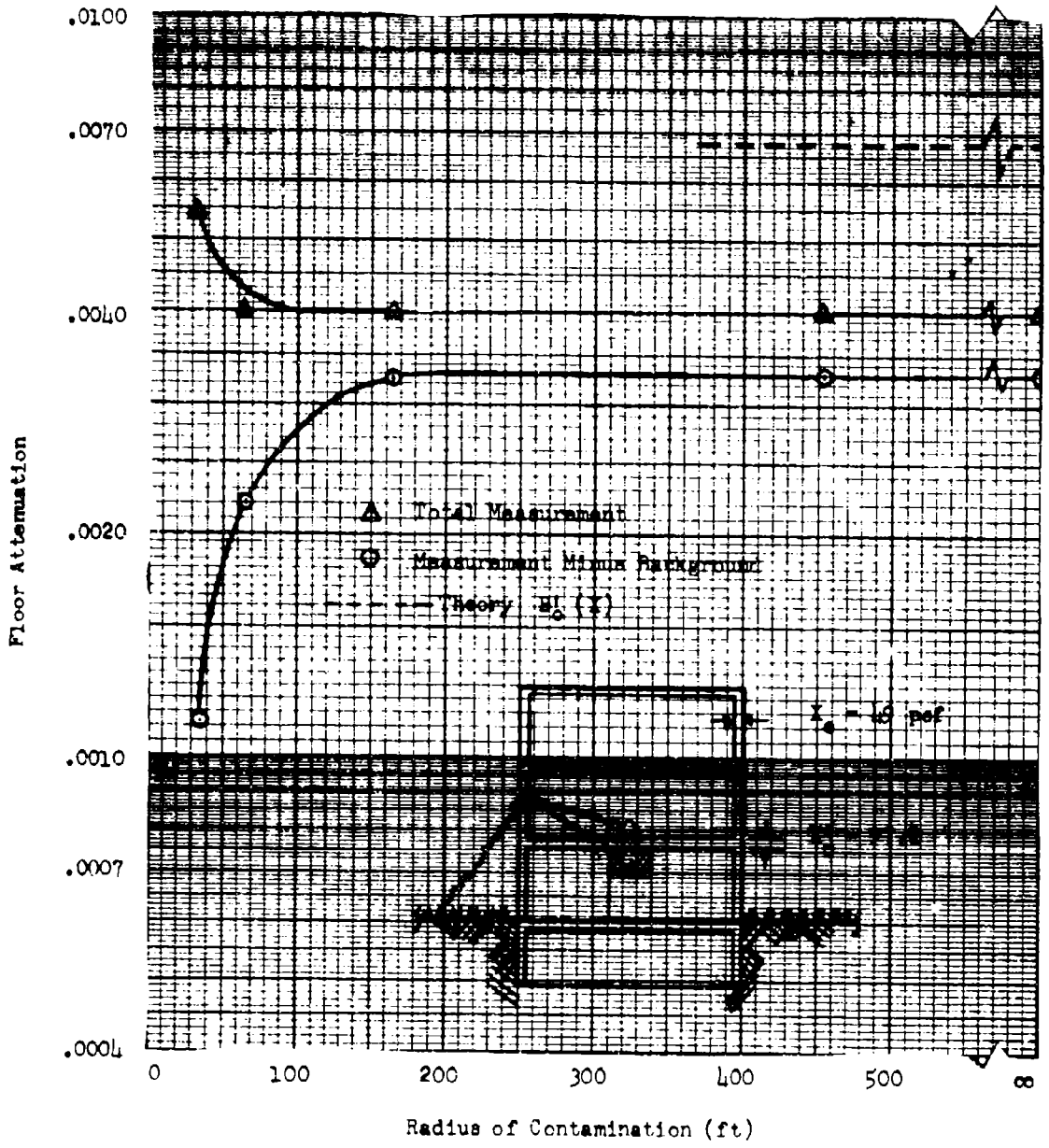

Comparison of Experimental and Calculated "In and Down" Floor Barrier Factor $B'_o(X_o)$ as Measured Above Ground for Cobalt-60

Figure 5.13

TABLE 5.3

Experimental Results of an "In-And-Up" Radiation Component

(First-Story Ceiling of Multistory Structure)

$D = (r/hr)/(curie/ft^2)$

Area	48.6 psf Ceiling		97.2 psf Ceiling	
	Above Floor D_A	Below Floor D_B	Above Floor D_A	Below Floor D_B
I	0.312	3.62	0.053	3.37
II	0.153	3.76	0.043	3.72
III	0.081	2.95	0.011	3.14
IV	0.056	1.46	0.0079	1.67

Radius of Contamination (ft)	D_B/D_A 48.6 psf Ceiling	D_B/D_A 97.2 psf Ceiling
0 to 32	.087	.016
0 to 64	.063	.013
0 to 164	.053	.010
0 to 452	.052	.0097

the building. The floor-mass thicknesses for this experiment were 48.6 and 97.2 psf. The walls were kept constant at 49 psf. These data are shown in the form of floor factors $B_f(X_f)_{exp}$ in Fig. 5.14 as a function of radius of contamination.

The theoretical function $B_f(X_f)$ is shown in Fig. 5.14 as a solid curve. Again this function, like the "in-and-down" function $B'_o(X'_o)$, is determined only for an infinite field of contamination and, hence, appears as a straight line on this graph. As was previously stated, the floor mass is assumed to attenuate "in-and-up" radiation similar to the L(X) function calculated by Spencer. This assumption would appear to be conservative because L(X) was calculated for an infinite uniformly-contaminated plane, while it is used here in a situation in which there is a cleared area (building plan area) directly below the detector, the location of the most penetrating radiation. As expected, the results shown in Fig. 5.14 plainly illustrate this conservatism. The calculated functions represent an underestimation of the attenuation afforded by the 48.6 psf barrier by 35 percent and the 47.2 psf barrier by 80 percent. For close-in limited fields of contamination (less than 100 feet), the calculated function is much less conservative and, in fact, in the case of the 48.6 psf barrier, was non-conservative.

6. CONCLUSIONS AND RECOMMENDATIONS

6.1 GENERAL

The purpose of this study was to investigate experimentally one of the known problem areas ("in-and-down" radiation component) that exists in fallout shielding technology. Also, an attempt was made to include all reported past experiments and modifications to the existing technology. Because of the variations of geometry and structural compositions in all of the experimental buildings reported to date, it was not possible to make a direct comparison with theory.

6.2 CONCLUSIONS

General conclusions of this study are listed below:

1. The relative agreement between experimental and calculated reduction factor curves in the center of a basement without a ceiling is good.

2. For structures with basement ceilings, the calculated reduction factor curves do not agree with experimental curves, and

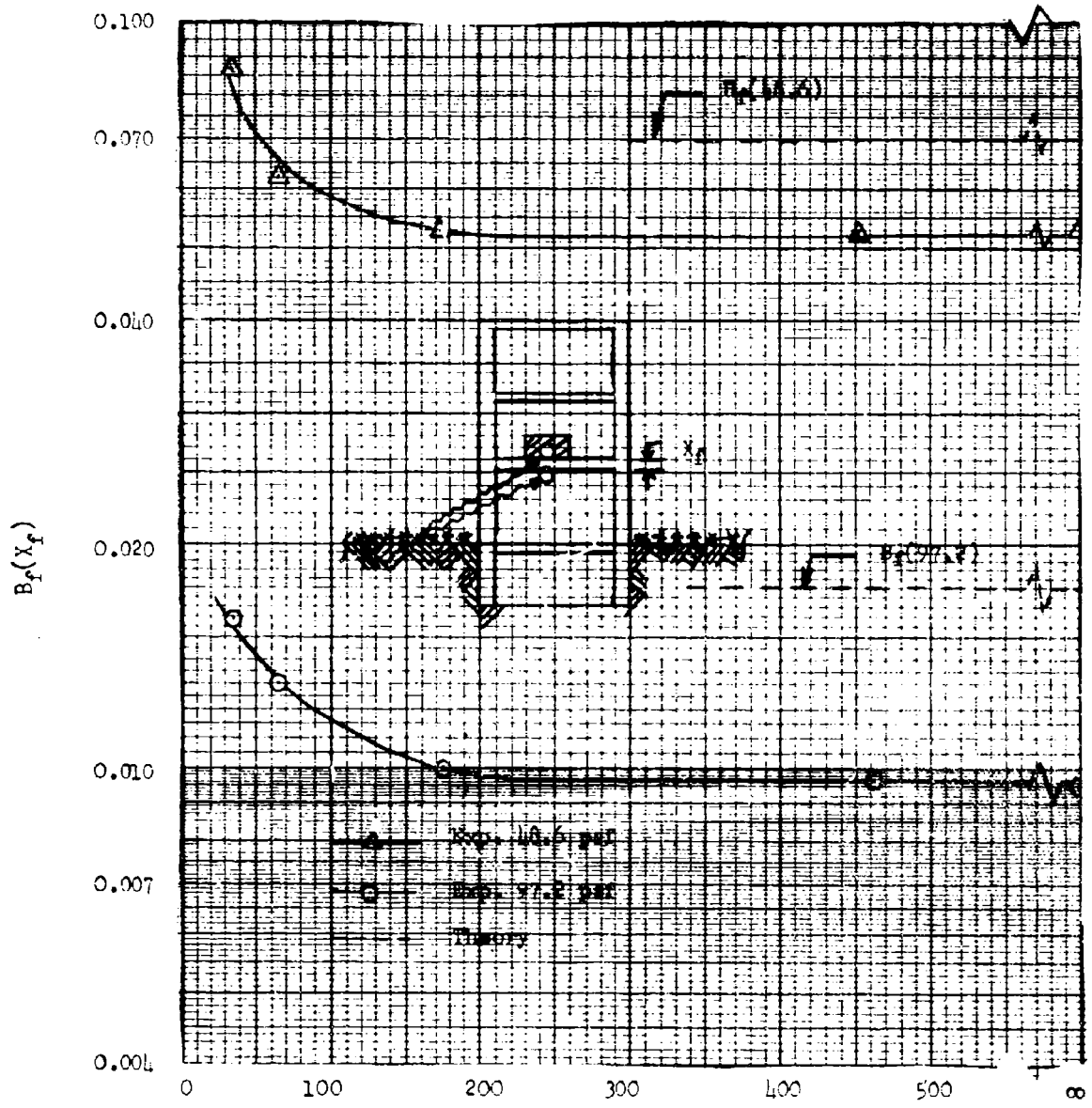

Radius of Contaminated Field (ft.)

Comparison of Experimental and Calculated "In and Up" Attenuation by a Floor Barrier for Cobalt-60

Figure 5.14

can represent an underestimation of the dose received in the basement by as much as a factor of three. The discrepancy between theory and experiment increases with decreasing solid-angle fraction.

3. The calculated horizontal barrier factor $B'_b(X'_b)$ is within 35 percent of the experimental barrier factor for the two mass thicknesses investigated, with the calculated value representing an underestimation of the attenuation afforded by the barriers. Note that this applies to slab attenuation only.

4. The modification to the method used in OCD PM-100-1, proposed by Batter, in which the ceiling attenuation is a function of the mass thickness of the ceiling barrier and a geometry term based on energy loss and scattering from the exterior vertical wall, $B'_b(X,\Omega)$, while conservative agrees with the experimental results as function of solid-angle fraction.

5. The calculated barrier factor $B'_b(X'_b)$ represents an underestimation of attenuation afforded by floors in upper stories because of radiation scattered in the downward direction.

6.3 RECOMMENDATIONS

The following recommendations are offered as a result of this study:

1. A new function, similar perhaps to the function $B'_b(X_o\Omega)$, calculated by Batter[12] for floor attenuation, should replace the function $B'_b(X'_b)$ in the functional equation for predicting reduction factors in basements of structures.

2. A further study of basement ceiling attenuation should be undertaken, utilizing an idealized experimental configuration that can be used to systematically investigate each parameter in the calculated method.

3. An experimental and analytical investigation of the effect of non-uniform floors (e.g., caused by the steel floor support beams) on the dose rates in basement areas should be undertaken. The results of this study indicates that the beams that supported the ceiling slabs in the basement were responsible for considerable reduction in basement area dose rates.

REFERENCES

1. Spencer, L.V., Structure Shielding Against Fallout Radiation from Nuclear Weapons, NBS Monograph 42, June 1962

2. OCD PM 100-1, The Design and Review of Structures for Protection from Gamma Radiation, February 1965

3. OCD, Shelter Design and Analysis, TR-20, Vol. 2, October 1964

4. Eisenhauer, C., An Engineering Method for Calculating Protection Afforded by Structures Against Fallout Radiation, NBS-76, July 1962

5. Batter, J.F., and Starbird, A.W., Attenuation of Cobalt-60 Radiation by a Simple Structure With a Basement, Technical Operations, Inc., TO B-61-39, July 1961

6. Study of the Radiation Distribution Within a Multistory Structure from Finite and Infinite Plane Sources of Contamination, PSDC TR-24 (unpublished)

7. Batter, J.F., et al, Final Report on the Effect of Limited Strips of Contamination of the Dose Rate in a Multistory Windowless Building, Technical Operations, Inc., TO B-62-58, August 1962

8. Batter, J.F. and Starbird, A.W., The Preparation of Simplified Manuals for Shielding Analysis, CONESCO 4848-1, March 1967

9. Batter, J.F., etal, The Barrier Attenuation Introduced by a Vertical Wall, PSDC-TR-15, September 1964

10. McDonnell, C.A., et al, Description, Experimental Calibration, and Analysis of the Radiation Test Facility at the Protective Structures Development Center, PSDC-TR-14, September 1964

11. Private Communication, M. Schmuchyk, NDL, September 1966

12. Batter, J.F. and Starbird, A.W., The Preparation of Simplified Manuals for Shielding Analysis, Supplement No. 1, Final Report, CONESCO 4848-2, March 1967

REFERENCES
(Continued)

13. LeDoux, J.C., Ceiling-Shine Contribution Within Buildings from Fallout Radiation Field, USNCEL Technical Study No. 30 in Atomic Defense Engineering, February 1963

APPENDIX A

EXPERIMENTAL DATA

The experimental data reported in this study were obtained using Victoreen Model 362, 200 mr; Model 229, 10 mr; or Model 208, 1 mr, non-direct-reading ionization chambers (dosimeters), together with a Technical Operation Model 556 Charger-Reader. Dosimeter selection was based upon the expected exposure time, the area of the field being simulated, the thickness of the floors, and the location of the dosimeter with respect to the contaminated area.

All dosimeters and the charger-reader were calibrated against a gamma source of known strength and National Bureau of Standards calibrated Victoreen R meters. Dosimeters selected for this experiment responded to within ±2 percent of the known dose. The chambers were also checked at intervals during the experiment, using a secondary calibration procedure.

All dosimeter readings were normalized to specific dose rate; that is, to a per-hour basis for an equivalent contamination density of one curie of Cobalt-60 per square foot (1 curie Cobalt-60 = 14.0 r/hr at 1 ft at STP). This is the source density required to produce a radiation field of 464 r/hr three feet above an infinite smooth uniformly-contaminated plane. Dosimeter readings were converted to a r/hr basis, using dosimeter calibration constants, exposure time, source strength, and temperature-pressure corrections for the effect of atmospheric conditions. The equation used to normalize these readings in roentgens to specific dose rates in $(r/hr)/(curie/ft^2)$ is

$$I = \frac{DA}{t S_o} \qquad (A\text{-}1)$$

where D = measured dose normalized to standard atmospheric conditions (Roentgens)

A = area of the contaminated field (ft^2)

S_o = source strength (curies)

t = exposure time (hrs)

I = specific dose rate in $(r/hr)/(curie/ft^2)$

The experimental data are tabulated in this Appendix in terms of normalized specific dose rate and reduction factors. Table A-1 shows the data obtained for the structure with zero psf floors. Table A-2 presents the data for the structure with 48.6 and 97.2 psf floors. All data are presented as a function of the depth below ground and the solid-angle fraction subtended at the detector by the basement ceiling.

TABLE A-1

Basement Radiation Measurement Dose Rates and Reduction Factors

Depth (ft)	Solid-Angle Fraction ω_u	Area 1 0 - 32'	Area 2 32'-64'	Area 3 64'-164'	Area 4 164'-452'	Far-Field Dose	Total Dose D_1	Reduction Factor D_1/D_o
		Wall Thickness 49 psf Floor Thickness 0 psf						
-2.0	0.87	3.24	4.22	4.16	3.63	2.06	17.31	.037
-3.0	0.81	2.59	3.19	3.36	2.81	1.60	13.55	.029
-4.0	0.75	2.28	2.66	2.96	2.44	1.38	11.72	.025
-5.0	0.70	2.04	2.43	2.68	2.16	1.22	10.53	.023
		Wall Thickness 98 psf Floor Thickness 0 psf						
-2.0	0.87	1.42	1.62	1.66	1.22	.692	6.612	.014
-3.0	0.81	1.05	1.27	1.27	1.02	.58	5.19	.011
-4.0	0.75	.976	1.10	1.12	.90	.512	4.608	.0099
-5.0	0.70	.864	1.00	1.01	.824	.468	4.166	.0089
		Wall Thickness 147 psf Floor Thickness 0 psf						
-2.0	0.87	.484	.544	.568	.42	.238	2.254	.0049
-3.0	0.81	.404	.412	.416	.312	.177	1.721	.0037
-4.0	0.75	.376	.372	.351	.27	.153	1.522	.0033
-5.0	0.70	.356	.344	.322	.237	.135	1.394	.003

Dose Rates In (R/hr) / (Curie/ft^2)

TABLE A-2

Basement Radiation Measurement Dose Rates and Reduction Factors

Depth (ft)	Solid-Angle Fraction ω_u	Area 1 0 - 32'	Area 2 32'-64'	Area 3 64'-164'	Area 4 164'-452'	Far-Field Dose	Total Dose D_T	Reduction Factor D_T/D_o
Wall Thickness 49 psf Floor Thickness 48.6 psf								
-2.0	0.87	.0744	.14	.151	.139	.0788	.5832	.0013
-3.0	0.81	.11	.189	.212	.184	.105	.80	.0017
-4.0	0.75	.115	.189	.216	.213	.121	.854	.0018
-5.0	0.70	.128	.184	.212	.184	.105	.813	.0018
Wall Thickness 49 psf Floor Thickness 97.2 psf								
-2.0	0.87	.0114	.0232	.0209	.0144	.0092	.0781	.00016
-3.0	0.81	.017	.026	.0277	.021	.0119	.1036	.00022
-4.0	0.75	.0195	.0272	.0308	.034	.0193	.1308	.00028
-5.0	0.70	.0228	.0277	.0305	.0228	.0130	.1168	.00025
Wall Thickness 98 psf Floor Thickness 97.2 psf								
-2.0	0.87	.00576	.0064	.008	.0078	.00444	.0324	.000069
-3.0	0.81	.0096	.00892	.0112	.0078	.004444	.04196	.00009
-4.0	0.75	.0116	.00952	.0121	.0112	.00632	.05074	.0001
-5.0	0.70	.017	.00972	.0121	.017	.00964	.06546	.00014

Dose Rates in (R/hr) / (Curie/ft^2)

APPENDIX B
ERROR ANALYSIS

The test of reproducibility of experimental data is not necessarily indicative of true experimental error because, in this procedure, only random errors are considered. Both random and systematic errors must be considered to determine the true accuracy of this experiment.

Ideally, a precise analysis of the error associated with this experiment would proceed by randomizing all systematic errors, determining the standard deviation of each error, and compounding these standard deviations according to accepted statistical rules to determine the standard deviations of the final experimental result. Unfortunately, randomization of all the systematic errors is not practical, nor is determination of the standard deviation for each variable warranted. The approach used has been to determine experimentally or to estimate, on the basis of knowledge and experience with the methods used, the standard deviation for each variable contributing to the final result, and then to compound these standard deviations according to the accepted principles.

Some of the systematic errors present in these experiments cancel. The ones that cancel will be determined by the kind of experiment considered (i.e., finite or infinite sources of contamination), and the way in which the data are presented (e.g., as reduction factor, specific dose rate, or direct attenuation factor).

In general, the results of the experiments described in this report are presented in specific dose rates, and the ratio of specific dose rates and attenuation factors. The specific dose rate is related to the variables in the experiment by the data normalization equation as

$$D = \frac{mAT}{10^3 PCSt} \qquad (B\text{-}1)$$

where D = specific dose rate in r/hr/curie/ft^2

m = charger-reader microamp reading

A = simulated source area

T = temperature in degrees Rankine

P = pressure in inches of H_g

C = charger-reader calibration constant

t = source exposure time in hours

S = source strength in curies

The standard deviation of each of the variables is related to the standard deviation of the specific dose rate by total differential of the normalizing equation

$$\Delta D = \left[\frac{\partial D}{\partial m} \Delta m + \frac{\partial D}{\partial T} \Delta T + \cdots \frac{\partial D}{\partial A} \Delta A \right] \qquad (B-2)$$

or, in percentages, the standard deviation is given by

$$\left(\frac{\sigma D}{D}\right)^2 = \left[\left(\frac{\sigma m}{m}\right)^2 + \left(\frac{\sigma T}{T}\right)^2 + \cdots\cdots \left(\frac{\sigma A}{A}\right)^2\right] \qquad (B-3)$$

Thus, the percentage errors may be simply squared and added.

A. Measurement Errors - The estimated or measured standard deviations of each of these variables for all types of experiments are considered to be as follows:

The Simulated Source Area A. Since the tubing was laid out quite carefully for these relatively large areas, this error is negligible ($\sigma A/A < 0.1\%$).

Source Strength S_o. The error in the reduction factor values caused by an error in source strength cancels only if the same sources are used in the same areas for both the determination of the infinite-field normalization value and all other infinite-field experiments. This does not generally occur. Although all source strengths were determined using NBS calibrated Victoreen chambers and charger-reader, there are inherent errors in source-to-detector distances and air-density determinations. A standard deviation of 2 percent for source strength can be estimated other than any systematic error that will cancel in the normalization to reduction factor.

Microamp Reading μa. The following are incorporated into the microamp standard deviation. The dosimeter group variation value has been determined experimentally.

(1)	Scale reading error		0.5
(2)	Normal 96% dosemeter group variation		0.5
	so that	σm =	1.0

Temperature, T, in Degrees Rankine

(1)	Scale reading error		0.5°
(2)	Time variation		2.5°
	so that	σT =	3.0°

Pressure, P, in Inches of Hg

(1)	Scale reading		0.01 in.
(2)	Time variation		0.01 in.
	so that	σP =	0.02 in.

Charger-Reader Calibration Constant C

The error in reduction factor resulting from error in the calibration constant does not cancel unless the same charger-reader is used to determine the infinite-field normalization value, as well as all other experimental values. The standard deviation has been estimated experimentally to be less than two percent for any combination of charger-readers.

Time of Source Runs in Hours (t)

Since the timing is done visually, with a stop watch, the error is principally that of reaction, since

$$\sigma t = 1 \text{ sec}$$

$$\sigma t = 0.0003 \text{ hr}$$

B. Errors Associated with Infinite-Field Normalization Value

Most experimental results are given as reduction factors which require that the specific dose rate resulting from an experiment be divided by the normalization value D_o, which is the specific dose rate three feet above an infinite smooth plane of contamination. D_o was experimentally determined to be 464 r/hr/curie/ft^2 for an infinite uniformly-contaminated plane of Co-60. This experimental value is essentially the result of five experiments, one for each simulated area, so that a representative case for each experiment will be considered separately. In addition to compounding the standard deviations resulting from the five experimental areas[10], error contributions from the ground roughness and far-field correction factors will also be included in the final estimate of the standard deviation for the infinite-field normalization value.

Area OA - Building Plan Area (Fig. 4.2)

A	= 247.0 ft^2	σ_A/A	= 0.1%
S	= 5.25 curies	σ_S/S	= 2%
t	= 0.15 hr	σ_t/t	= 0.2%
C	= 8.48	σ_C/C	= 2%
m	= 63.0	σ_m/m	= 1.6%
T	= 520°R	σ_T/T	= 0.6%
P	= 30.00 H_g	σ_P/P	= 0.1%

From Equation (B-3)

$$\sigma_{oo}/D_{oo} = \left[4 + 0.04 + 4 + 2.56 + 0.36 + 0.01\right]^{1/2}$$

$$= \left[10.97\right]^{1/2} = 3.31\%$$

$$D_{oo} = 39.86 \text{ r/hr/curie/ft}^2$$

$$\sigma_{oo} = 1.32 \text{ r/hr/curie/ft}^2$$

Area 1A - Building Plan Area to 32-foot Radius (Fig. 4.2)

A	= 552.0 ft^2	σ_A/A	= 0.1%
S	= 5.2[illegible] curies	σ_S/S	2%
t	= 0.94 hr	σ_t/t	= 0.1%
C	= 8.48	σ_C/C	= 2%
m	= 62.0	σ_m/m	1.6%
T	= 498°R	σ_T/T	= 0.6%
P	= 30.00 in. H_g	σ_P/P	= 0.1%

From Equation (B-3)

$$\frac{\sigma_{1A}}{D_{1A}} = \left[4 + 4 + 2.56 + 0.01 \right]^{1/2} = \left[10.93 \right]^{1/2} = 3.31\%$$

Since D_{1A} = 13.41 r/hr/curie/ft^2

σ_{1A} = 0.45 r/hr/curie/ft^2

Area 2A - 32-Foot Radius to 64-Foot Radius (Fig. 4.2)

A	= 2828.0 ft^2	σ_{2A}/A	= 0.1%
S	= 52.8 curies	σ_S/S	= 2%
t	= 0.391 hr	σ_t/t	= 0.1%
C	= 8.48	σ_C/C	= 2.0%
m	= 57.0	σ_m/m	= 1.8%
T	= 523°R	σ_T/T	= 0.6%
P	= 30.00 in. H_g	σ_P/P	= 0.1%

From Equation (B-3)

$$\sigma_{2A}/D_{2A} = \left[4 + 0.01 + 4 + 3.24 + 0.36 + 0.01 \right]^{1/2}$$

$$= \left[11.67 \right]^{1/2} = 3.41\%$$

Since $D_{2A} = 16.4$ r/hr/curie/ft^2

$\sigma_{2A} = 0.56$ r/hr/curie/ft^2

Area 3A - 64-Foot Radius to 164-Foot Radius (Fig. 4.2)

A	= 17492 ft^2	σ_A/A	= 0.1%
S	= 52.8 curies	σ_S/S	= 2%
t	= 2.01 hr	σ_t/t	= 0.1%
C	= 8.48	σ_C/C	= 2%
m	= 50.0	σ_m/m	= 2%
T	= 515°R	σ_T/T	= 0.6%
P	= 30.29 in. Hg	σ_P/P	= 0.1%

From Equation (B-3)

$$\sigma_{3A}/D_{3A} = \left[4 + 4 + 4 + 0.36 + 0.01\right]^{1/2} = \left[12.37\right]^{1/2} = 3.52\%$$

Since $D_{3A} = 16.38$ r/hr/curie/ft^2

$\sigma_{3A} = 0.58$ r/hr/curie/ft^2

Area 4A - 164-Foot Radius to 452-Foot Radius (Fig. 4.2)

A	= 139357 ft^2	σ_A/A	= 0.1%
S	= 538.0 curies	σ_S/S	= 2%
t	= 1.785 hr	σ_t/t	= 0.1%
C	= 8.48	σ_C/C	= 2%
m	= 46.0	σ_m/m	= 2.0%
T	= 515.0°R	σ_T/T	= 0.6%
P	= 30.30 in. Hg	σ_P/P	= 0.1%

From Equation (B-3)

$$\sigma_{4A}/D_{4A} = \left[4+4+4.5+0.36+0.01\right]^{1/2} = \left[12.87\right]^{1/2} = 3.59\%$$

Since $D_{4A} = 13.37$ r/hr/curie/ft^2

$\sigma_{4A} = 0.46$ r/hr/curie/ft^2

Far-Field Correction

The far-field correction factor, determined analytically, is used to estimate the effects of a field of contamination extending from the outermost radius (452 feet) of that simulated to infinity. To estimate the effect of this "missing" contamination, it is assumed that the dose buildup factor, point source to point detector, near a ground-air interface, may be adequately represented by a polynomial expansion of the form $B(\mu x) = 1 + 0.55\mu x$. To evaluate this assumption, we may estimate the amount of "far-field radiation" using various methods of approximation. The fraction of the total dose rate above an infinite field represented by contamination beyond a 452-foot radius: (1) may be determined from the experimental data of Rexroad[1], (2) may be computed using the results of the moments calculation of Spencer[2], (the dose rate above the center of a cleared circle is expressed by Spencer as $L(x)$, where x is the slant distance from the edge of the circle to the detector), or (3) may be computed by summing point source to the point detector values using $B(\mu x) = 1 + 0.55\mu x$ as the dose buildup factor. The third method is used in this report. The results of this manipulation for two altitudes typical of the minimum and maximum investigated in this study are illustrated in Table B-1. The estimate of far-field contribution used in this report agrees somewhat better with the experiments of Rexroad[1] than with the calculation of Spencer. The reason for this may be attributed to the fact that Spencer's moment calculations were performed in an infinite medium neglecting the effect of the density interface. This lack of density interface effect is expected to over-emphasize the scattered dose contribution

from the far-field region. The maximum difference in these correction factors is seven percent. This value is used as an estimate of the maximum error in the far-field correction factor. The percentage of standard deviation of the far-field contribution is

$$\frac{\sigma_{FA}}{D_{FA}} = \left[\left(\frac{\sigma_{4A}}{D_{4A}}\right)^2 + \left(\frac{\sigma_{FF}^2}{D_{FF}}\right)\right]^{1/2} = \left[\left(3.59\right)^2 + \left(7.0\right)^2\right]^{1/2} = 7.9\% \qquad \text{(B-4)}$$

TABLE B-1

Fraction Of Infinite Field Dose Rate Attributable To Contamination Beyond 452-Foot Radius And The Ratio Of That Dose Rate To That Attributable To The Region Extending From 164 to 452-Foot/Radius

Height	Fraction	Date of Reference	Ratio
3	.08	Rexroad[6]	0.56
3	.11	Spencer[5]	0.65
33	.19	Spencer[5]	0.65
3	.082	This report	0.57
33	.157	This report	0.58

Total Standard Deviation for D_o

The results for each of the five areas and the far-field value must be summed and multiplied by four (because of quarter symmetry) to find the total specific dose rate at three feet. This result must be multiplied by a ground roughness correction factor of 1.08 to arrive at the infinite field D_o value. The ground roughness factor, determined by fitting an experimental curve to a theoretical one[3], is assumed to be accurate to about three percent. If D is the total specific dose rate at three feet, and G is the ground roughness correction, then

$$D_o = DG \qquad (5)$$

where

$$\sigma_D = (\sigma_{oo}^2 + \sigma_{1A}^2 + \sigma_{2A}^2 + \sigma_{3A}^2 + \sigma_{4A}^2 + \sigma_{FA}^2)^{1/2} \qquad (B\text{-}6)$$

$$\sigma_D = 7.1 \text{ r/hr/curie/ft}^2$$

or

$$\frac{\sigma_D}{D} = \frac{7.1}{429} = 1.66\%$$

and

$$\frac{\sigma_G}{G} = 3\%$$

so that the total standard deviation expressed as a percent is

$$\frac{\sigma_{D_o}}{D_o} = \left[1.66^2 + 3^2\right]^{1/2} = 3.4\%$$

C. Experiments Using the Infinite Field

It can be assumed that the standard deviations of specific dose rates determined from the simulated infinite-field source are the same as that of the infinite-field D_o normalization value. When these specific dose rates are reduced to reduction factors, the systematic error of the ground roughness correction factor in the ratio cancels. If D is any specific dose rate from the infinite field, and R is the reduction factor, D/D_o, the percentage of standard deviation is

$$\frac{\sigma_R}{R} = \left[\left(\frac{\sigma_D}{D}\right)^2 + \left(\frac{\sigma_{D_o}}{D_o}\right)^2\right]^{1/2} \qquad (B\text{-}7)$$

and

$$\frac{\sigma R}{R} = \left[1.7^2 + 1.7^2\right]^{1/2} = 2.5\%$$

For reduction factors determined within the test structure, the effect of the nominal wall thickness values must be considered. For this analysis, the mass thickness effect upon the reduction factor may be represented adequately as an exponential, so that

$$R_x = R \cdot e^{-x/x_o} \qquad \text{(B-8)}$$

where x is the wall thickness in psf and x_o is the psf corresponding to one mean free path.

From Equation (B-2)

$$\Delta R_x = \frac{\partial R_x}{\partial R} \Delta R + \frac{\partial R_x}{\partial x} \Delta x$$

or $$\Delta R_x = e^{-x/x_o} \Delta R - \frac{R\, e^{-x/x_o} \Delta x}{x_o}$$

so $$\frac{\Delta R_x}{R_x} = \frac{\Delta R}{R} - \frac{\Delta x}{x_o}$$

and $$\frac{\sigma R_x}{R_x} = \left[\left(\frac{\sigma R}{R}\right)^2 + \frac{x}{x_o}\left(\frac{\sigma x}{x}\right)^2\right]^{1/2} \qquad \text{(B-9)}$$

It has been determined[3] that the standard deviation of the wall panels used with the test structure is about 9.5 pounds. The standard deviation for reduction factor can be determined from the above equation.

$$\frac{\sigma R_x}{R_x} = \left[(2.5)^2 + \frac{48.6}{36.3}(1.3)^2\right]^{1/2} = 2.9\%$$

D. Experiments With Finite Fields

The experiments reported here are concerned with measurement of radiation from finite sources of contamination. These measurements can be treated in a manner similar to that applied to a single area in the open-field analysis.

Assuming that the percentage of standard deviation in the specific dose rate for a finite field is represented by the Area 00 Fig. 4.2), value of 3.31 percent, the analysis proceeds as follows:

Reduction factor

$$R = \frac{D_{oo}}{D_o}$$

$$\left(\frac{\sigma R}{R}\right)^2 = \left(\frac{\sigma D_o}{D_o}\right)^2 + \left(\frac{\sigma D_{oo}}{D_{oo}}\right)^2$$

or

$$\left(\frac{\sigma R}{R}\right)^2 = (3.4)^2 + (3.3)^2$$

$$\frac{\sigma R}{R} = 4.7\%$$

This percentage of standard deviation for reduction factors due to finite fields is representative of the experiments considered in this report. An additional error is associated with the random variations of the weight of the concrete slabs used. Fifteen of these concrete roof panels were selected at random, measured, and weighed to establish their mass thickness. The dimensions of these panels varied by about +1/16-inch from the basic dimensions, introducing an uncertainty of approximately 0.25 percent. These panels were weighed using a Baldwin load cell calibrated to one part in a thousand against a known mass of water. Each slab was weighed in turn, producing weights varying from 735 pounds to 761 pounds. The

average slab weight was determined as 744 pounds, with a standard deviation of 9.5 pounds, or 1.3 percent. Expressed as a mass thickness, this is 48.6 psf with $x = 0.6$ psf. The effect of this variation is closely represented, as in the infinite-field experiments, by $R_x = R_e^{-\lambda x}$, where x is the [illegible]

$$\left(\frac{\sigma R_x}{R_x}\right)^2 = \left(\frac{\sigma R}{R}\right)^2 + \frac{\lambda}{x_o} \left(\frac{\sigma x}{x}\right)^2$$

$$\frac{\sigma R}{R_x} = \left[(4.7)^2 + \frac{48.6}{36.3} (1.3)^2\right]^{1/2} = 5.7\%$$

Reduction factors from these experiments can, therefore, be expected to have a percentage of standard deviation of 5.7 percent.

E. Additional Error Due to Source Asymmetry

A possible additional error, which has been ignored in the preceeding analysis, is that of the source asymmetry. Because of the cylinder construction of the source capsule, source intensity is less in directions parallel to the axis of the cylinder. The sources used have been calibrated with directions perpendicular to the axis of the cylinder. This additional error in the specific dose rate D_o has been ignored, since a detector in the standard positions views the end of the source only a small percentage of the time.

F. Conclusions

The analsyis shows that when the systematic error of the ground roughness correction does not cancel in an experiment, it is the most dominant error. This is the case for the infinite-field D_o value and the finite-field reduction factors. When the ground roughness effects are negated by the normalization, it has been shown that the dominant errors are those due to source strength,

charger-reader calibration constants and the charger-reader microamp reading (which incorporates errors due to the 96 percent dosimeter group variation, as well as the scale-reading error).

Table B-2 summarizes the results of this analysis in terms of estimated standard deviation and the probable error ($p = 0.67\,\sigma$)

TABLE B-2

Major Experimental Errors

Type of Experiment	Estimated Percent Standard Deviation	Probable Error
Infinite-Field D_o	3.4%	2.3%
Infinite-Field D	3.4%	2.3%
Infinite-Field Reduction Factor	2.9%	1.9%
Finite-Field D	3.5%	2.4%
Finite-Field Reduction Factor	5.7%	3.8%

REFERENCES - APPENDIX

1. Rexroad, R., and Schmoke, M., Scattered Radiation and Free-Field Dose Rates From Cobalt-60 and Cesium 13, NDL-TR-2, September 1960

2. Spencer, L.V., Structure Shielding Against Fallout Radiation From Nuclear Weapons, NBS Monograph 42, June 1962

3. McDonnell, C.H., et al, Description, Experimental Calibration, and Analysis of the Radiation Test Facility at the Protective Structures Development Center, PSDC-TR-14, September 1964

UNCLASSIFIED

Security Classification

DOCUMENT CONTROL DATA - R&D

(Security classification of title, body of abstract and indexing annotation must be entered when the overall report is classified)

1 ORIGINATING ACTIVITY (Corporate author)
Protective Structures Development Center
Building 2590, Fort Belvoir, Virginia 22310

2a REPORT SECURITY CLASSIFICATION
UNCLASSIFIED

2b GROUP

3 REPORT TITLE
A PRELIMINARY INVESTIGATION OF "IN-AND-DOWN" AND "IN-AND-UP" RADIATION COMPONENTS

4 DESCRIPTIVE NOTES (Type of report and inclusive dates)
Final Report

5 AUTHOR(S) (Last name, first name, initial)
Velletri, Joseph D.

6 REPORT DATE	7a TOTAL NO OF PAGES	7b NO OF REFS
October 1966	88	13

8a CONTRACT OR GRANT NO	9a ORIGINATOR'S REPORT NUMBER(S)
DA-18-020-ENG-3407	PSDC-TR-25
b PROJECT NO	
c	9b OTHER REPORT NO(S) (Any other numbers that may be assigned this report)
d Subtask 1117A	

10 AVAILABILITY/LIMITATION NOTICES
Distribution of This Document is Unlimited

11 SUPPLEMENTARY NOTES	12 SPONSORING MILITARY ACTIVITY
	Department of the Army Office of the Secretary of the Army Office of Civil Defense

13 ABSTRACT

An experiment was designed to measure the attenuation afforded by horizontal barriers both above and below ground to radiation that originated from sources lying on the ground surrounding a structure. Measured attenuation factors in the downward direction (in-and-down) agreed fairly well with calculated factors for the two barrier-mass thicknesses (486. and 97.2 psf) investigated.

The observed dose rates in the basement of the ceilingless structure agreed fairly well with the existing theory, while large discrepancies between theory and experiment were found in the experiment dealing with the structure basement which had a ceiling. This discrepancy increased with decreasing solid-angle fraction with the theory underestimating the dose rate in the basement by as much as a factor of 3. The experimental results were consistent with past experiments conducted in basement structures in their comparison with theory. A modification to the theory in which a new barrier factor was calculated as a function of the barrier thickness and average solid-angle fraction subtended at the detector by the first-floor external wall agrees quite well with this experiment and past experimental results.

The calculated attenuation factors in the upward direction (in-and-up radiation component) underestimated the experimental results for large or infinite fields of contamination, and over-estimated the attenuation afforded by the floor from contamination within 50 feet of the structure walls.

DD FORM 1 JAN 64 1473

Security Classification

KEY WORDS	LINK A		LINK B		LINK C	
	ROLE	WT	ROLE	WT	ROLE	WT
Basement, Protection Factors						
Radiation Shielding						
Concrete Attenuation - Gamma Radiation						
Reduction Factors						
Fallout, Simulated Field						
"In-and-Up" and "In-and-Down" Gamma Radiation Components						

INSTRUCTIONS

1. ORIGINATING ACTIVITY: Enter the name and address of the contractor, subcontractor, grantee, Department of Defense activity or other organization (*corporate author*) issuing the report.

2a. REPORT SECURITY CLASSIFICATION: Enter the overall security classification of the report. Indicate whether "Restricted Data" is included. Marking is to be in accordance with appropriate security regulations.

2b. GROUP: Automatic downgrading is specified in DoD Directive 5200.10 and Armed Forces Industrial Manual. Enter the group number. Also, when applicable, show that optional markings have been used for Group 3 and Group 4 as authorized.

3. REPORT TITLE: Enter the complete report title in all capital letters. Titles in all cases should be unclassified. If a meaningful title cannot be selected without classification, show title classification in all capitals in parenthesis immediately following the title.

4. DESCRIPTIVE NOTES: If appropriate, enter the type of report, e.g., interim, progress, summary, annual, or final. Give the inclusive dates when a specific reporting period is covered.

5. AUTHOR(S): Enter the name(s) of author(s) as shown on or in the report. Enter last name, first name, middle initial. If military, show rank and branch of service. The name of the principal author is an absolute minimum requirement.

6. REPORT DATE: Enter the date of the report as day, month, year, or month, year. If more than one date appears on the report, use date of publication.

7a. TOTAL NUMBER OF PAGES: The total page count should follow normal pagination procedures, i.e., enter the number of pages containing information.

7b. NUMBER OF REFERENCES: Enter the total number of references cited in the report.

8a. CONTRACT OR GRANT NUMBER: If appropriate, enter the applicable number of the contract or grant under which the report was written.

8b, 8c, & 8d. PROJECT NUMBER: Enter the appropriate military department identification, such as project number, subproject number, system numbers, task number, etc.

9a. ORIGINATOR'S REPORT NUMBER(S): Enter the official report number by which the document will be identified and controlled by the originating activity. This number must be unique to this report.

9b. OTHER REPORT NUMBER(S): If the report has been assigned any other report numbers (*either by the originator or by the sponsor*), also enter this number(s).

10. AVAILABILITY LIMITATION NOTICES: Enter any limitations on further dissemination of the report, other than those imposed by security classification, using standard statements such as:

(1) "Qualified requesters may obtain copies of this report from DDC."

(2) "Foreign announcement and dissemination of this report by DDC is not authorized."

(3) "U. S. Government agencies may obtain copies of this report directly from DDC. Other qualified DDC users shall request through _____."

(4) "U. S. military agencies may obtain copies of this report directly from DDC. Other qualified users shall request through _____."

(5) "All distribution of this report is controlled. Qualified DDC users shall request through _____."

If the report has been furnished to the Office of Technical Services, Department of Commerce, for sale to the public, indicate this fact and enter the price, if known.

11. SUPPLEMENTARY NOTES: Use for additional explanatory notes.

12. SPONSORING MILITARY ACTIVITY: Enter the name of the departmental project office or laboratory sponsoring (*paying for*) the research and development. Include address.

13. ABSTRACT: Enter an abstract giving a brief and factual summary of the document indicative of the report, even though it may also appear elsewhere in the body of the technical report. If additional space is required, a continuation sheet shall be attached.

It is highly desirable that the abstract of classified reports be unclassified. Each paragraph of the abstract shall end with an indication of the military security classification of the information in the paragraph, represented as (*TS*), (*S*), (*C*), or (*U*).

There is no limitation on the length of the abstract. However, the suggested length is from 150 to 225 words.

14. KEY WORDS: Key words are technically meaningful terms or short phrases that characterize a report and may be used as index entries for cataloging the report. Key words must be selected so that no security classification is required. Identifiers, such as equipment model designation, trade name, military project code name, geographic location, may be used as key words but will be followed by an indication of technical context. The assignment of links, rules, and weights is optional.